

KfK 3059
September 1980

Modification of the Superconducting and Structural Properties of Ion Implanted and Ion Irradiated Transition Metals and Transition Metal Compounds

G. Linker, J. Geerk, O. Meyer, J. Pflüger
Institut für Angewandte Kernphysik

Kernforschungszentrum Karlsruhe

ION IMPLANTATION IN SUPERCONDUCTORS

O. MEYER

Kernforschungszentrum Karlsruhe GmbH Institut für Angewandte Kernphysik I, Postfach 3640,
D-7500 Karlsruhe 1, Federal Republic of Germany.

(Paper first read at the International Conference on Ion Beam Modification of Materials, September 4-8, 1978, Budapest, Hungary).

I INTRODUCTION

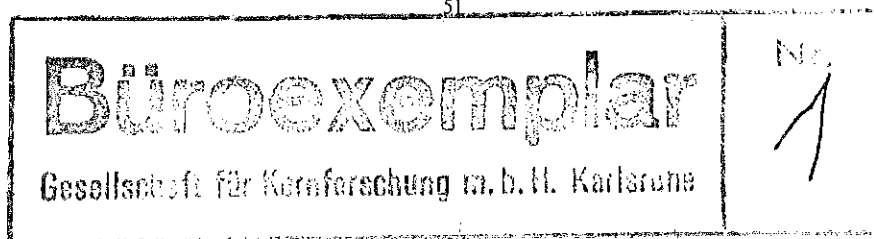
Ever since its discovery by Kamerlingh Onnes in 1913 superconductivity has attracted many workers, theorists as well as experimenters, in order to understand this interesting physical phenomenon and to discover new superconductors with improved properties useful for applications. On the experimental side this search has led to the discovery of nearly stoichiometric Nb_3Ge ^{1,2} with the highest superconducting transition temperature T_c of 23.2 K presently known and to the discovery of the Chevrel phases with critical magnetic fields of about 60 Tesla.³

On the theoretical side the basic mechanism namely the electron-phonon interaction leading to pairing of electrons and thus to superconductivity has been described by Bardeen, Cooper and Schrieffer⁴ and with this mechanism many of the experimental results could be explained. Considering strong coupling effects T_c is given by:⁵ $T_c \sim \langle \omega \rangle \exp(-(1 + \lambda)/\lambda)$, where $\langle \omega \rangle$ is the average phonon frequency and λ the electron-phonon coupling constant given by: $\lambda = N(O)\langle I^2 \rangle / M\langle \omega^2 \rangle$. $N(O)$ is the electronic density of states at the Fermi energy, $\langle I^2 \rangle$ is an electronic matrix element and M is the atomic mass. Despite of the progresses in theory it is still difficult to predict the superconducting properties of complex materials. There seem however to be general arguments from both theory and experiment that a further increase of T_c may be achieved if materials with enhanced phonon softening (decrease of $\langle \omega^2 \rangle$) and high density of electronic states $N(O)$ can be realized. This goal is difficult to reach however from the metallurgical point of view as there are severe obstacles such as solubility limits, lattice instabilities followed by phase transitions, equilibrium compositions in compounds far

from optimum stoichiometric compositions and the lack of long range ordering. In order to overcome these difficulties numerous experiments have been performed using non-equilibrium preparation techniques such as splat-cooling, chemical vapour deposition, quench condensation, co-evaporation, sputtering and ion implantation.

In the following review examples will be presented which clearly demonstrate that ion implantation in many respects is superior to other non-equilibrium techniques mentioned above. In particular advantages and disadvantages of the application of ion implantation to different material classes revealing interesting superconducting properties will be discussed. Many elements show enhanced T_c -values if they are strongly distorted or if they are transferred to an amorphous phase. Results of implanted disordered systems will be presented in Chapter II. Metastable ion implanted alloys with interesting superconducting properties have been produced as will be shown in Chapter III. Well ordered systems such as the A15 compounds for example have the highest T_c -values if their structure is undistorted and the long range order parameter approaches unity. In such structures radiation damage will strongly depress T_c and up to now ion implantation is of limited success for the preparation of the A15 compounds. Nevertheless ion implantation has also been used for the formation and improvement of ordered compounds. Such experiments, especially implantation into niobium and vanadium carbides will be described in Chapter IV. A short summary of applications using ion implantation is presented in Chapter V.

Numerous studies were concerned with the influence of neutron and light ion radiation damage on the superconducting critical current and critical field. A summary of this work up to



1968 is given by Cullen.⁶ Further developments in this field including work on heavy ion implantation effects are covered in the Proceedings of the International Discussion Meeting on Radiation Effects on Superconductivity.⁷ Results on ion implantation effects in superconductors have been summarized in Ref. 8, a review on the production metastable superconducting phases is given in Ref. 9. The present contribution emphasizes studies performed using heavy ions, where considerable changes of the metallurgical state of the material occur.

II DISORDERED SYSTEMS

a Non-transition Metals

Many elements can be rendered amorphous or stabilized in a highly disordered state by quench condensation, that is the evaporation onto substrates cooled with liquid He.¹⁰ The metallurgical state of these vapour quenched films is difficult to analyze in detail. It may range from small crystallites, with short range order preserved in a microcrystalline structure, the so-called lattice-like amorphous state, to a phase where the short range order is different from the crystalline phase. In this second phase the coordination number is higher and thus the amorphous phase is more metallic similar to the liquid, therefore this phase is called liquid-like amorphous.¹¹ These disordered phases which usually will recrystallize by warming up to room temperature very often exhibit enhanced T_c -values. It has been found that a higher degree of disorder is stabilized by co-evaporating impurities and some elements can be stabilized in an amorphous phase only by the addition of impurities. An excellent review on amorphous metals and their superconductivity is given by Bergmann.¹²

Well-known example of such a superconductor is Al with a bulk T_c -value of 1.2 K. All films prepared by quench condensation show enhanced T_c -values of 3.3 K.¹¹ Quench condensation in the presence of O₂, H₂ and rare gases results in T_c -values between 2 and 4.5 K.¹⁵ Co-evaporation of Ge or Si with Al onto substrates at liquid He temperature yielded films reaching 6.0 and 6.6 K, respectively.^{13,14} Again the microscopic structure is decisive for the possible T_c -enhancement mechan-

TABLE I

Maximum T_c -values as observed after implantation of various ions in Al thin films at 4 K^{17,19}

Implanted ion	He	C	O	Al	Si	Ge	H	D
max T_c	3.7	4.2	4.0	2.6	8.35	7.35	6.75	6.05

ism. In quenched Al-films the increase of T_c is generally ascribed to a softening of the phonon spectrum caused by lattice disorder. In Al-films with stabilizing elements incorporated, a granular structure consisting of small Al grains separated by semiconducting or insulating barriers has been observed at room temperature.¹⁴ Based on the idea of this granular structure T_c -enhancement mechanisms such as changes in the amplitude of the electron-phonon interaction,¹⁴ by excitonic¹⁵ or surface plasmon¹⁶ effects have been suggested.

Implantation of various ions in Al-films below 10 K have been performed in order to obtain more detailed information about the T_c -enhancing mechanisms.^{17,18} The T_c -values obtained in these experiments are summarized in Table I.

Implantation of Si and Ge in Al-films exhibits T_c -values of 8.35 K for Al₆₀Si₄₀ and of 7.35 K for Al₆₀Ge₄₀. These T_c -values are considerably larger than those obtained by co-evaporation onto cold substrates. By implantation of He (and O-ions) T_c increases to about 4 K, a value similar to those found by quench condensation. Al-ion implantation resulted in a T_c -value of 2.6 K. A further exciting result is the high T_c -value of 6.75 K observed after H-implantation in Al-films. In this special case there are several hints that an ordered compound has been produced. Firstly additional implantation of a low fluence of Al-ions was found to reduce T_c to about 4 K indicating that additional disorder destroys the high T_c -phase and leads to T_c -values observed for O- and He-implantation. Secondly, resistivity results¹⁷ of a high dose H-implanted Al-sample suggest that H-ordering or phase transformation takes place. The formation of an ordered AlH₂ compound is likely to occur as the average H-concentration implanted in Al is close to this composition. Tunneling experiments¹⁸ have shown an enhanced electron attraction due to coupling via acoustical phonons. As changes of the phonon spectrum are not observed, the T_c -enhancement is proposed to be due to an increase of the electron-phonon-coupling

parameter $\alpha^2(\omega)$ caused by hydrogen influencing the electronic properties.

The results obtained for He, C and O implanted Al-films have been explained by phonon softening due to lattice disorder similar to the T_c -enhancement mechanism in quenched Al-films. The T_c -enhancement found after the implantation of Al-ions suggested that intrinsic damage is present. The question whether this T_c -enhancement is due to intrinsic damage or disorder stabilized by impurities has been studied²⁰ by Al-ion implantation and irradiation of Al thin films with various oxygen content at temperatures below 4 K. The results from this work are presented in Figure 1.

Figure 1a shows the T_c -variation for low Al-fluences where the collision cascades do not yet overlap and mainly point defects prevail. In Figure 1b the results for high Al-fluences are presented. Here both, specific resistivity ρ , and T_c -variations are found to correlate with the oxygen content in the films. In contrast to the results given in Table I, Al-implantation into pure Al-films with a residual resistivity ratio ($R_{RT}/R_{2.5K}$) of about 11 does not lead to an increase of T_c .

A T_c -value of 2.6 K as given in Table I however is reached by Al-implantation into Al-films having an oxygen content of about 4 at. % corresponding to a residual resistivity ratio of about 3.5. The dependence of the T_c -values on the residual gas content of the as-condensed Al-films shows that additional disorder is stabilized by the impurities during irradiation.

The T_c -enhancing mechanism, causing the exceptionally high T_c -values for Si and Ge implanted Al-films is still in debate. For both $Al_{1-x}Si_x$ and $Al_{1-x}Ge_x$ the transition from metallic to semi-conducting conduction occur for $x \geq 0.45$, the maximum T_c -values are obtained for $x \approx 0.4$ with $\rho \approx 100 \mu\Omega\text{cm}$ indicating extremely high damage levels.²¹

After annealing an Al-Si film up to room temperature T_c was found to decrease to 3.3 K. Additional irradiation with Si with fluences of 2×10^{15} ions/cm² at 6 K was found to increase T_c sharply back to the original value of 8.3 K. This experiment demonstrates that disorder is important and some disorder is still retained at room temperature. From the similarity of the

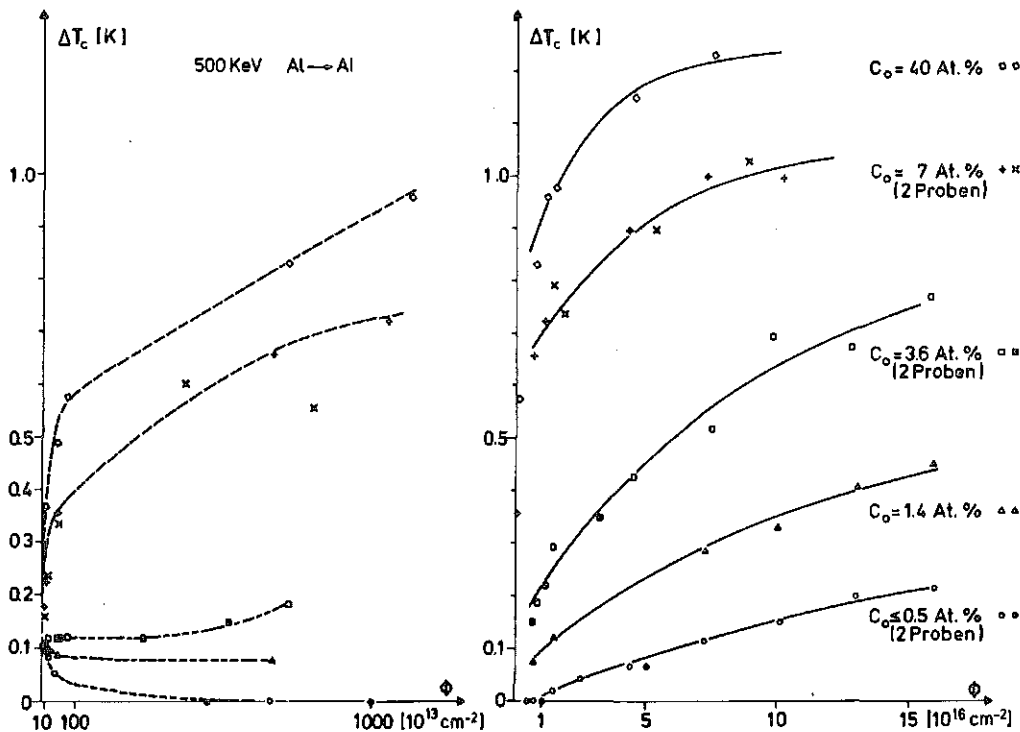


FIGURE 1 T_c variations of thin Al films with various oxygen content as a function of Al-ion fluence (a) for low Al-ion fluence, (b) for fluences above $10^{16} \text{Al}^+/\text{cm}^2$ (21).

dependence of T_c and ρ on composition between implanted films and granular structures an increase of the electron-phonon interaction matrix element has been suggested as a common interpretation of the T_c -enhancement mechanism.²¹

With regard to the possible contribution of Si and Ge to the T_c -enhancement there exist interesting results for quench condensed and ion implanted Ge noble metal alloys. Quench condensed Ge-films are still semiconducting, revealing a lattice-like amorphous phase. By co-deposition of Ge together with a noble metal (Cu, Ag or Au) onto a liquid He-cooled substrate a superconducting phase is stabilized having a maximum T_c -value of 3.3 K for $\text{Ge}_{50}\text{Cu}_{50}$.²² Recent electron diffraction investigation²³ on quenched Ge-noble metal alloys at 4 K however show broad diffraction rings similar to those of liquid Ge. From this experiment one may conclude that the enhanced superconductivity is due to a liquid like amorphous phase of Ge and is not due to a granular structure.

Implantation of Cu-ions at 4 K in pure Ge and Ge-Cu alloy films as well as irradiation of these films with Kr-ions have been performed in order to answer the question if Ge or Cu is responsible for superconductivity.²⁴ The maximum T_c -value reached in these implantation experiments is 3.7 K, i.e. about 0.4 K higher than observed for quenched alloy films. As the maximum T_c -value occurs already at 25% Cu it is concluded that Ge is responsible for the superconductivity. The Cu-atoms stabilize the lattice disorder and prevent Ge from the formation of covalent Ge—Ge bonds. This means that in this case a higher degree of lattice disorder can be produced with ion implantation than by quench condensation.

b Transition Metals

The influence of disorder on the T_c -values of transition metals (TM) and TM-alloys produced by vapour deposition onto cryogenic substrates has been studied in Ref. (25). In general a decrease of T_c was found in disordered films of the group Vb TM (V, Nb, Ta) and an increase of T_c was observed for group VIb and VIIb (Mo, W, Re). In contrast to disorder in non-transition metals (NTM) where annealing to 100 K is in most cases sufficient to remove the lattice disorder, higher annealing temperatures are necessary for the recrystallization of disordered TM systems. The important role of impurities in stabilizing disordered phases in

quench condensed Mo and Nb-layers has been described recently in Ref. (26).

Heavy ion implantation and irradiation of TM-films also resulted in substantial variations of T_c .²⁷ Strong T_c depressions have been observed in evaporated V-, Nb- and Ta-layers, whereas T_c -enhancements were found in Mo, W and Re thin films. As impurity-stabilized disorder will not anneal at room temperature it is difficult to separate the influence of alloying effects on T_c from that of disorder produced during implantation and irradiation of oxygen contaminated TM-films. The importance of impurities present in a layer for changes of T_c under ion bombardment has been recognized in experiments with ion implantation into Mo-layers at temperatures below 10 K.²⁸ Here the observed increase of T_c after irradiation with noble gas ions was found to correlate with the oxygen content in the as-evaporated Mo-layers. For oxygen concentrations below about 1 at.% resulting in Mo-layers with a residual resistivity greater than 4, no T_c was detected down to 1.7 K even after high fluence Xe-ion irradiation. In Mo-layers with an oxygen content of about 8 at.% increases from 1.7 to 7.7 K were observed depending on Xe-fluence. Implantation of O-ions resulted in a T_c^{max} value of 5 K, additional irradiation of the implanted layers with Xe-ions causes a further enhancement up to 7.7 K. From these results it was concluded that disorder is stabilized by oxygen and that the stabilization is more effective if the density of mobile defects in a single collision cascade is increased by using heavier ions (Xe instead of O or Ne). Disorder in Mo stabilized by oxygen recrystallized by warming up to 200°. For this reason O-stabilized disorder will not be produced during O-implantation at room temperature in agreement with experiment.

The implantation of chemically active impurities with electronegativity values greater than that of Mo into pure Mo-films has been found to increase T_c .²⁸ A summary of these results is given in Table II.

Maximum T_c -values reached were 9.2 K for N-implantation at a concentration of 23 at.%, for S at 22 at.% and for P at 27 at.%. Figure 2 shows the increase of T_c as a function of implanted N-ion concentration at liquid He and room temperature. From the maximum T_c -values of 9.2 and 7.0 K, respectively, it is seen that annealing takes place for room temperature implantation.

As the same T_c -maximum of 9.2 K has been found after implanting different ions this value is

TABLE II

Maximum T_c -values and corresponding saturation values of the concentration after implantation of various ions in Mo thin films at 4 K.²⁸

Ion	B	C	N	O	Ne	Al	P	S	As	Sb	Bi	Xc
T_c^{max}	8.7	8.3	9.2	4.5	<1.7	<1.7	9.2	9.2	7.6	1.7	<1.7	<1.7
at. %	16	17	23	10	20	35	27	25	30	35	35	20

attributed to a disordered Mo-phase. The nature of this high T_c -phase for the system Mo-N has been studied in more detail,²⁹ especially as it could be argued that molybdenum nitride compounds may be formed and are responsible for the T_c -enhancement. The high T_c -values observed for N-implantation into Mo at temperatures below 10 K could be correlated with a highly disordered bcc Mo-phase. During annealing fcc as well as fcc crystallographic structures appeared while the T_c -value decreased continuously as a function of annealing temperature. Finally at 850°C T_c decreased below 1.2 K while the fcc-phase was still present. The decrease of T_c and the structural transformations as a function of temperature in an isochronal annealing process are summarized in Figure 3 for samples implanted at liquid He- and at room temperature. The stabilization of the disordered high T_c -phase in these experiments is therefore ascribed to the interaction of the chemically active impurity atoms with the distorted host lattice as no such effects were observed either with bombardment or implantation of noble gas ions in pure Mo. From channeling measurements

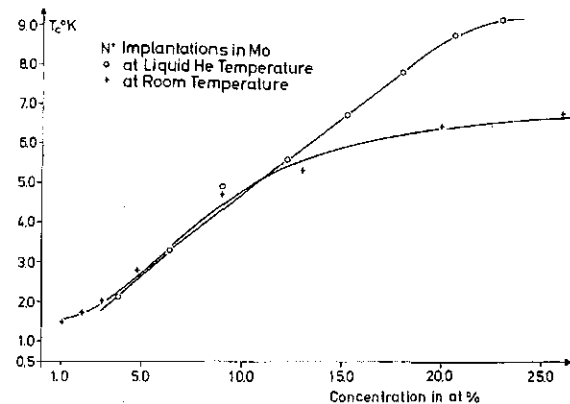


FIGURE 2 Increase of T_c as a function of implanted nitrogen concentration for liquid He- and room-temperature implantations. Maximum observed T_c -values were 9.2 and 7.0 K respectively for these temperatures.³¹

it was concluded that Mo-lattice is completely disordered for a N-concentration of about 23 at. % in agreement with the concentration value necessary to reach the maximum T_c -value.

The influence of impurities on the depression of T_c in heavy ion implanted and irradiated vanadium layers was studied in Ref. (36). Vanadium layers have been produced with various oxygen contents analyzed by Rutherford backscattering allowing an oxygen concentration determination down to about 0.2 at. %. Implantations and irradiations were performed using Ne- and N-ions at room temperature. The T_c -values of as-evaporated layers were in the range of 4.9 to 5.25 K, nearly independent of the oxygen concentration up to 6 at. %. For higher oxygen contamination levels reduced T_c -values have been observed. Figure 4a shows the relative T_c -decrease in pure V-layers implanted with N-ions as a function of N-concentration. In Figure 4b the relative T_c -depression in oxygen contaminated V-layers irradiated with

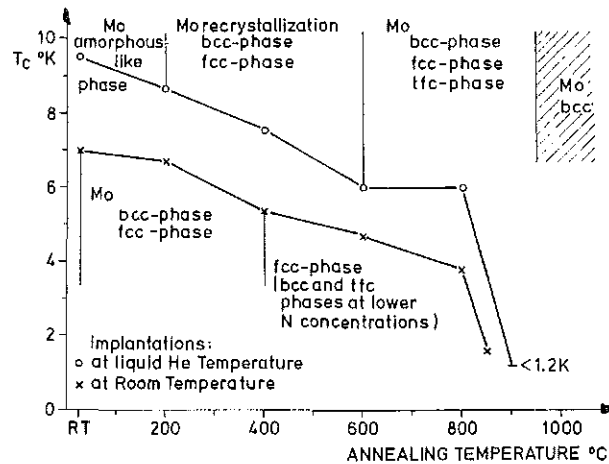


FIGURE 3 Decrease of the superconducting transition temperature T_c and structural transformations as a function of temperature in an isochronal (1 h) annealing process. Samples were implanted till T_c -saturation at liquid He-temperature and with 33 at. % nitrogen at room temperature, respectively.³¹

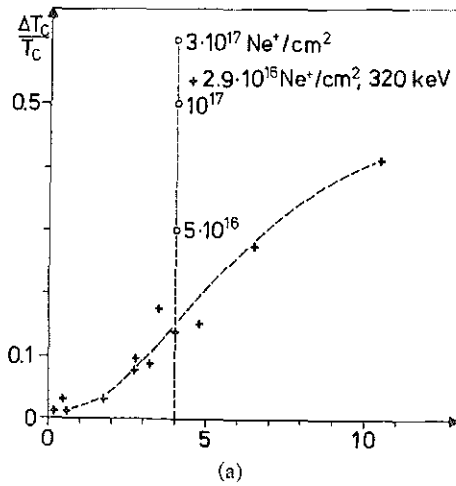


FIGURE 4a Relative decrease of T_c as a function of implanted N-ion concentration in V-layers.³⁵

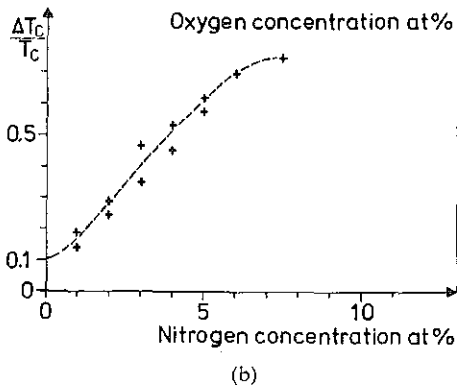


FIGURE 4b Relative decrease of T_c of V-layers with various oxygen content after irradiation with 2.9×10^{16} Ne/cm² at 320 keV. For a V-layer with 4 at. % oxygen the relative decrease of T_c is shown with the Ne-ion fluence as a parameter. At about 3×10^{17} Ne/cm² $\Delta T_c/T_c$ is found to saturate at 0.6, about the same amount as observed after implanting 4 at. % N as can be seen in Figure 4a.³⁷

2.9×10^{16} Ne⁺/cm² at 320 keV as a function of oxygen concentrations is shown. For a V-layer with 4 at. % oxygen the T_c -decrease with the Ne-fluence as parameter is included in Figure 4b.

The following conclusions were drawn from these results: chemically active impurities play an important role in the T_c -decreases. These impurities can be either implanted into the layer or activated, i.e. moved from oxide precipitates into the vanadium grains by recoil implantation during irradiation with noble gas ions. As similar T_c -depressions have been obtained with O- and N-implantations it is unlikely that this effect is

caused by alloying as N is almost insoluble in V. It is assumed that the T_c -decrease is due to disorder in the host lattice itself. The structure of this disorder is not completely clear, channeling experiments show that locally displaced V-atoms are present in V single crystals implanted with N under similar conditions as the layers. X-ray analysis of the nitrogen implanted V-layers showed that the V bcc structure is only slightly disturbed and that the lattice parameter has increased. In Table III results from implantation and irradiation experiments in pure and oxygen contaminated V- and Mo-layers with Ne- and N-ions are summarized.

The important role of chemically active impurities on the stabilization of the disordered phases in transition metal layers with enhanced or decreased T_c -values is clearly demonstrated in this summary.

III METASTABLE ALLOYS

a Magnetic Impurities in Non-transition Metals

Magnetic atoms have been dissolved in NTM to investigate the influence of localized moments on the electronic properties of the host. From the dependence of T_c and the specific resistivity ρ on the impurity concentration, information is obtained about the coupling of localized moments and the conduction electrons of the host. The slope of the T_c -depression is a direct measure of the pair breaking parameter.³¹ Such experiments are difficult to perform mainly for two reasons: the solubility limit of elements from the iron group in non-transition elements is usually very low (e.g. 100 ppm for Mn in Sn and below 100 ppm for Mn in Pb). In order to enhance the solubility quench condensed alloys have been produced. For quench condensed alloys however an unknown amount of lattice defects will be frozen in. The presence of lattice defects will influence the slope of the T_c -dependence as function of the solute concentration.

Ion implantation at liquid He-temperature has been used^{32,33} in order to overcome such difficulties. The solubility limit with the implantation technique is found to be much higher than in bulk alloys (about 1200 ppm for Mn in Pd). However implanted alloys are highly metastable and will anneal out at temperatures below 100 K. The influence of disorder on T_c could be separated by using non-magnetic ion species, e.g. Zn-ions of

TABLE III

Variation of T_c as result of implanted Ne- and N-ion fluence in pure and oxygen contaminated V- and Mo-layers.

Material		Implanted with	
		Ne ions	N ions
V $T_c = 5.2\text{K}$	Low oxygen content < 1 at. %	T_c -decrease low (few %)	T_c -decrease high (50% or more)
	High oxygen content few at. %	T_c -decrease high (below 1.2K)	T_c -decrease high (below 1.2 K)
Mo $T_c = 0.9\text{K}$	Low oxygen content < 1 at. %	no T_c above 1.7K	T_c -increase up to 9.2K
	High oxygen content few at. %	T_c -increase up to 5.5K at 4K	T_c -increase up to 9.2K

similar atomic mass and number as the paramagnetic Mn. A further advantage of ion implantation is the possibility to control concentrations in the ppm range with the same relative accuracy as at high concentration. Results from these implantation experiments³⁴ are presented in Figure 5, where it can be seen that small concentrations of Mn cause a strong depression of the T_c of homogeneously doped Hg, Pb and Sn-films. The slope of the curves is nearly constant at concentrations above 100 ppm in agreement with theory. At concentrations below 100 ppm a curvature in the T_c -curves can be seen, it is positive for the system Mn in Sn and negative for Mn in Pb and Hg. These deviations from the linear dependence reflect the influence of lattice defects on T_c as verified by implanting the nonmagnetic ions Cu and In into Pb- and Sn-layers respectively (see dashed curves in Figure 5). The same technique has been used for In-films implanted with Mn-ions³⁵ where the degree of lattice disorder has been varied by preimplantation of In-ions. In this way it was possible to explain differences in the amount of T_c -depression measured in quench condensed alloys of this system by different authors.

b Al-Based Alloys

The T_c -dependence on the concentration c of Ge, Zn and Mg alloyed with Al exhibits an interesting behaviour.³⁶ For concentrations below 1 at. % T_c decreases slightly in the range of a few percent independently of the nature (electronegativity,

valence, atomic size) of the solute. This decrease in T_c with concentration is ascribed to the removal of the anisotropy effect.³⁷ A further increase in concentration yields a positive slope dT/dc and the magnetic of this curvature was found to depend on the valence of the solute. At the solubility limits of 2 at. % for Ge, 25 at. % for Zn and 15 at. % for Mg, T_c saturates at 1.2, 1.6 and 1.45 K, respectively.³⁸

In order to see if ion implanted alloys reveal the same T_c -dependence on concentration and if an enhanced solubility will be reached, Ge, Zn and Mg-ions have been implanted into Al-films at

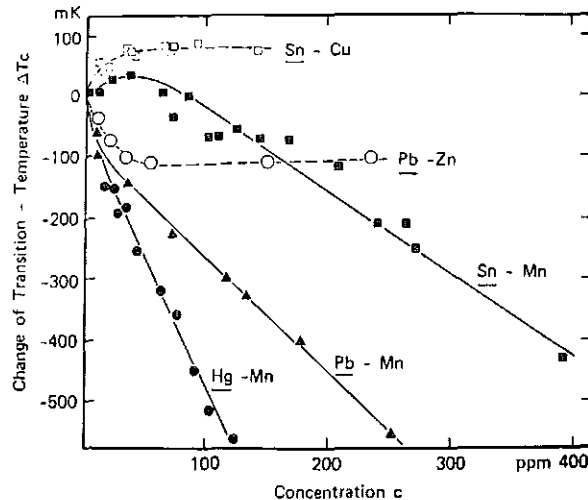


FIGURE 5 Variation of T_c after implanting Mn-ions in thin films of Hg, Pb and Sn. By implanting Cu-ions in Sn and Zn-ions in Pb the influence of disorder on T_c can be separated.³⁹

room temperature.⁸ In contrast to the findings observed for bulk alloys, ion implanted systems do not exhibit a decrease of T_c . An increase of T_c is observed in the concentration region from 0.001 to 20 at.%, with maximum T_c -values of 1.4 K, 1.42 K and 1.45 K, for Ge, Zn and Mg, respectively. Reasons for this difference in the T_c -dependence on concentration between ion implanted and bulk alloys may rise from disorder introduced during implantation at room temperature. This disorder is probably not completely annealed out and will influence T_c . In order to test this assumption, enhanced disorder has been introduced by implanting ions known to exhibit large size effects and also by implantation of ions which have large electronegativity values and which are not soluble in Al. Indeed, the highest T_c -increase has been observed for Ca, known to have the biggest size effect in Al and for C, S and N-ions known to have large electronegativity values. These results indicate, that the T_c -enhancement observed for various ions implanted in Al at room temperature is due to disorder and not to alloying. In Chapter II it was pointed out that disorder in Al-alloys produced by ion implantation at temperatures below 10 K does not completely anneal out when warming up to room temperature.

c Alloys with High Concentrations of Interstitials

An excellent demonstration for the usefulness of ion implantation becomes obvious from experiments in the Pd-H system.

This system was found to become superconducting for H/Pd ratios above 0.8.³⁹ Due to the limited solubility level with a maximum ratio H: Pd of 0.7 at one atm H₂ and 300 K, a high H-concentration is difficult to obtain. Therefore H- and D-implantations at liquid He temperature have been used to increase this ratio up to and above 1.⁴⁰ Maximum T_c -values of 9 K and 11 K were observed for nearly stoichiometric PdH and PdD, respectively. One of the main reasons for this T_c -increase is the suppression of spin-fluctuations of the Pd. It is known that the system becomes diamagnetic at a H/Pd ratio of about 0.7.

The question arose whether lattice disorder produced by the implantation process would have some effect on T_c . Therefore after the successful implantation experiments, efforts were made to produce stoichiometric PdH alloys by using high pressure or electrical H-charging at temperatures

of -50 to -80°C . The T_c -values obtained with the implantation technique have been confirmed. From these results it is concluded that defects produced during implantation either anneal out or do not influence T_c .

Further one may ask if the rather high T_c -values are mainly due to the Pd-matrix or to the interstitial H. Ion implantation has been used to solve this question as one can easily vary the implanted atom species. The following interstitial elements have been implanted in Pd and the maximum T_c -values obtained are given in brackets:⁴¹ H(8.8 K), D(10.7 K), B(3.8 K), C(1.3 K) and N(0.2 K). While an increase of T_c with mass is observed for H and D, the inverse isotope effect does not continue for the heavier elements. Through tunnel experiments⁴² it was shown that besides the suppression of the paramagnetism a further positive influence on T_c is due to an additional electron-phonon coupling with the optical H- and D-phonon modes.

If the Pd-matrix is changed by alloying with noble metals the solubility of H decreases rapidly and it becomes more difficult to apply other charging techniques besides ion implantation. Pd-noble metal alloys do not show superconductivity above 10 mK and becomes diamagnetic if the noble metal concentration exceeds 60 at.%. Foils with different noble and metal concentrations for the three systems Pd-Cu, Pd-Ag and Pd-Au have been produced and implanted with H-ions at 4 K⁴³ with increasing fluences until T_c passed the maximum. These maximum T_c -values are shown in Figure 6 as a function of the noble metal concentration

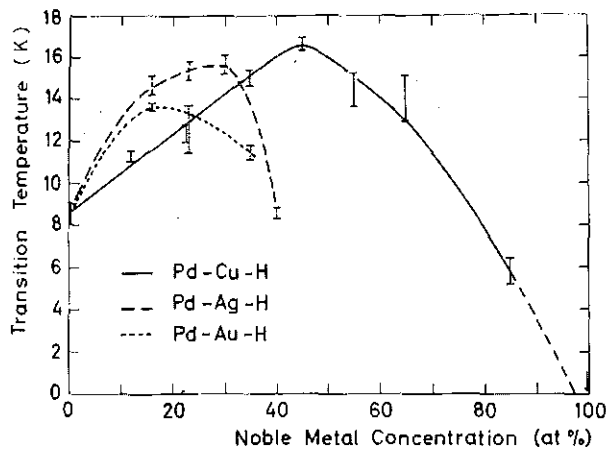


FIGURE 6 Maximum T_c -values observed after implanting H in Pd-noble metal alloys for various noble metal concentrations.⁴⁹

centration. The highest T_c of 16.6 K has been observed in the system H:Pd_{0.55}Cu_{0.45}. With increasing mass of the solute and with simultaneously increasing the H-content, T_c was found to decrease. This indicates that not only a closed-packed H-sublattice but also the matrix has a strong influence on the super-conductivity. The increase in T_c^{max} as a function of decreasing mass of the noble metal can be correlated with a softening of the acoustic phonon spectrum in agreement with results from neutron scattering experiments on hydrogenated PdAg alloy.⁴⁴

IV COMPOUNDS

a Refractory Compounds

The carbides and nitrides of the group Vb transition metals with NaCl crystal structure have interesting superconducting properties with high values of T_c , high critical magnetic field and high critical current density. The superconducting properties of the A15 compounds which will be discussed below are in general somewhat superior to those of the carbides and nitrides. However it has been shown that NbN and NbC are highly radiation resistant even against heavy ion bombardment in contrast to Nb₃Sn.²⁷ Therefore these materials seem to be well suited for ion implantation experiments.

The T_c -values of the carbides and nitrides are found to vary strongly with composition and reach a maximum value for the stoichiometric metal. In some cases such as VC, there is an appreciable deviation from the stoichiometric composition in the thermal equilibrium and it is not possible to form stoichiometric samples by thermal methods. Applying the diffusion method an almost stoichiometric niobium carbide with a C/Nb ratio of 0.98 and a T_c of 11.1 K has been obtained.⁴⁵

Ion implantation has been used in order to compensate deviations from stoichiometry. Results obtained by the diffusion technique have been compared to those obtained by C-ion implantation into NbC.⁴⁶ Single crystals of NbC_{0.89} were implanted at room temperature and at elevated temperatures (760° and 1070°C) with C-ions. In a second experiment a C-layer was evaporated onto a NbC_{0.89} single crystal and was diffused at temperatures between 1200 and 1600°C. The T_c -values were measured as a function of the annealing and diffusion temperature and the results are

shown in Figure 7. The dashed curve in Figure 7 shows the T_c -values of the carbon diffused single crystal as a function of diffusion temperature. T_c^{max} obtained in these diffusion experiments was 11.1 K in accordance with previous results.⁴⁵ After implantation of C-ions at room temperature T_c increased from 4 to 7 K. With increasing annealing temperature T_c increased and reached a maximum of 11.8 K. From this result it was concluded that a carbon content above 0.98 was reached by ion implantation. This assumption could be confirmed by backscattering measurements. A possible reason for the enhanced C-content is the comparatively low formation temperature of the implanted sample as compared to diffused samples causing a decrease of the equilibrium (vacancy) concentration.

The thermal equilibrium phase of vanadium has a C/V ratio of 0.89 and is not superconducting down to temperatures of 30 mK. This behaviour is exceptional in the group Vb carbides and nitrides and it has been explained with the low C/V atom ratio. Therefore C-ions were implanted into VC_{0.88} single crystals and the samples were examined for superconductivity.⁴⁷ None of the samples which were implanted at room temperature and subsequently annealed in an isochronal annealing process showed superconductivity. Increasing the sample temperature during implantation however resulted in superconductivity. The results of these experiments are shown in Figure 8. With increasing implantation temperature up to 800°C a maximum T_c -values of 3.2 K has been found. Higher implantation temperatures reduced T_c as carbon starts to diffuse out of the enriched layer. The implanted carbon profile and the carbon diffusion processes have been investigated applying the backscattering technique.⁴⁸

This example clearly demonstrates that ion implantation is a useful tool to compensate the deviations from stoichiometry beyond the thermal equilibrium composition.

b A15 Compounds

Compounds with the A15-structure such as Nb₃Sn (18.2 K) and V₃Ga (17 K) reveal the highest known T_c -values and the best performance in high field magnets up to now. Nb₃Ge (23.2 K) also belongs to this group of materials where the TM atoms are aligned and densely packed in three orthogonal chains and where the high T_c -values are thought to be caused by this chain

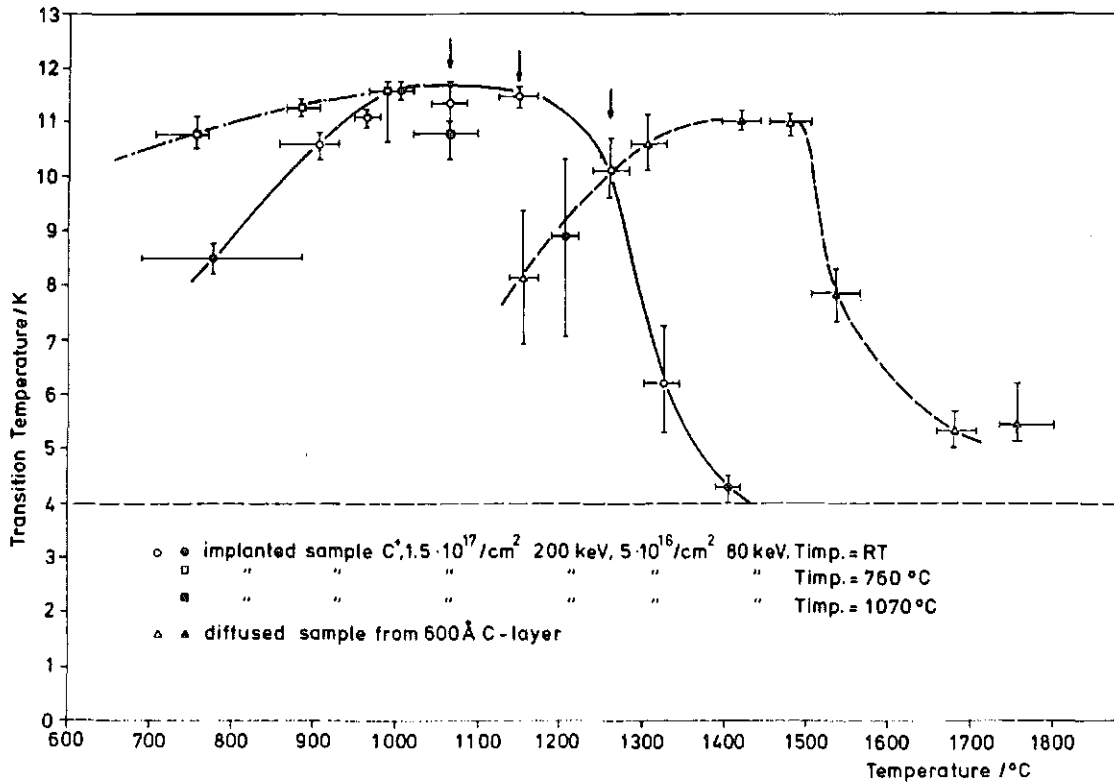


FIGURE 7 The transition temperature of a $\text{NbC}_{0.89}$ single crystal implanted with carbon ions (solid line) and with an evaporated carbon layer (dashed line) as a function of annealing and diffusion temperature, respectively. Also shown is T_c of a $\text{NbC}_{0.89}$ sample, implanted at 760°C as a function of annealing temperature (dashed-dotted line).¹⁵⁴⁾

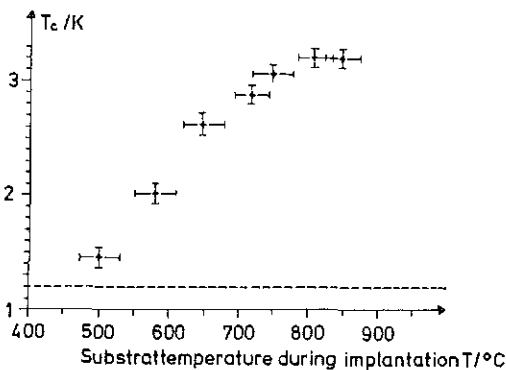


FIGURE 8 The transition temperature of $\text{VC}_{0.88}$ single crystals as a function of sample temperature during implantation of C-ions.⁵⁵⁾

structure. Any disorder in this structure will result therefore in a decrease of T_c . Inspection of the irradiated films with X-ray diffraction at fluences where the lower T_c -saturation has been just reached, revealed a small increase of the lattice

parameter.⁴⁹⁾ More detailed results on damage profiles and damage structures have been obtained by applying the channeling and back-scattering technique to the analysis of irradiated V_3Si single crystals.⁵⁹⁾ For crystals implanted with 300 keV He-ions a narrowing of the critical angle for the [100] as well as for the [110] channeling direction and an increase of the minimum yield has been observed as a function of He-ion fluence⁵⁰⁾ near the surface region. From these results which have been confirmed by Monte Carlo calculations followed that the V-atoms are displaced from their lattice sites with an average static amplitude of 0.06 \AA . A "zig-zag" arrangement of the atoms in the chain to release compression.

Implantations of Sn and Ge-ions into Nb thin films have been performed in order to study the formation of the A15 phase.⁵¹⁾ Two different types of experiments were performed to stabilize the A15-phase. Implantations were conducted at room temperature and subsequent annealing was carried

out at temperatures between 500 and 850°C. In a second experiment ions were implanted at high temperatures (650°, 725° and 800°C). The annealing temperatures required for the formation of the Nb₃Sn A15-phase was about 100° higher than from Nb-Sn sandwich films evaporated at 300 K. It is believed that lattice defects introduced during implantation hinder diffusion. T_c -values up to 17.8 K have been obtained after annealing of the implanted Nb-Sn system. Ge-implantations performed at various target temperatures and fluences followed by isochronal annealing treatments resulted in an A15-phase with T_c -values below 8 K. From these results it was concluded that ion implantation is probably not a useful technique to form or stabilize Nb₃Si which is believed to have a high T_c -values.

V APPLICATIONS

There are three main areas where the potentials of ion implantation for application are currently being explored. These areas are: (a) increase of pinning forces accompanied by an enhancement of surface current carrying capacity, (b) reduction of rf-losses at superconducting surfaces and (c) production of weak links.

For the production of pinning centers Nb foils with different oxygen contents have been bombarded with N- and O-ions at energies between 10 and 20 MeV and fluences in the range of 10^{12} and 3×10^{15} ions/cm².⁵² A significant increase of the critical current I_c and a slight increase in the upper critical field H_{c2} has been observed. Similarly after implanting Ni-ions at energies of 3.5 MeV into Nb-foils at 900°C a substantial increase in both I_c and H_{c2} has been found.⁵³ In both experiments voids have been observed in the implanted regions of the samples; these voids were believed to interact strongly with flux lines. Further experiments⁵⁴ have been performed implanting MeV Ni-ions into oxygen-doped Nb, NbZr and NbTa alloys, where dislocation loops as well as statistically distributed or regularly arranged voids have been observed. These defects acted as very effective pinning centers, and the elementary pinning forces are found to be larger than theoretical values calculated for possible interaction mechanisms.

Low frequency (30 Hz) losses have been measured in vanadium samples before and after implantation of Ga-ions. After implantation of

10^{16} Ga-ions per cm² at 75 keV a considerable reduction of the losses at lower amplitudes by two orders of magnitude have been observed due to a pronounced increase of the surface shielding capacity.

Ion implantation has attracted attention and lead to widespread use in modern microelectronics as its degree of precision for tailoring properties of thin films and surfaces in small dimensions is difficult to achieve by other means. There is an increasing interest to explore the possibilities of this technique for the production of superconducting weak link devices and microcircuits.

By implanting Fe-ions into a narrow band (5000 Å wide) across a strip of Nb thin films T_c is reduced and exceptionally stable weak links exhibiting the Josephson effects have been produced.⁵⁶ The critical current can be predetermined by controlling the number and location of the implanted ions. In a somewhat different procedure T_c has been increased up to about 4 K in a Mo-film by implanting N or S ions except a narrow band across the Mo-film which was covered with a photoresist mask during implantation this reducing the doping effect.⁵⁷ This slightly doped region with a T_c of about 1.7 K acts as a weak link between the heavily doped regions, and passes a super-current having an oscillatory diffraction pattern dependence on the magnetic field similar to that of Josephson tunnel junctions. Properties of ion implanted weak links are quite well described by recent theories⁵⁸ due to their well-defined geometry thus providing a basis for circuit design calculations. However, a number of significant improvements have to be worked out before such weak links will be useful for integrated circuits.⁵⁷

VI CONCLUSIONS

It is only about 7 years ago that the technique of ion implantation has been applied to improve the superconducting properties of materials. Within this short period of time very exciting results have been obtained which clearly demonstrate the advantages of this technique in material handling and modification. The T_c -dependence of the concentration of the solute element can be easily measured in one and the same sample whereby the reaction temperature can be optimized with regard to superconductivity. New and metastable alloys were produced as the concentration of the

solute can be raised above the equilibrium solubility limit. Compounds have been improved by compensating deviations in composition from stoichiometry. Disorder produced in such experiments can be annealed out by choosing reaction temperatures where intrinsic diffusion is small but not negligible. The influence of lattice defects on superconductivity can be studied in a very efficient way as intrinsic disorder effects can be separated from impurity stabilized disorder effects. Much remains to be learned about both the electronic and the structural properties of ion implanted layers. An increase in understanding in this respect, will certainly be followed by an improvement of superconducting properties.

REFERENCES

1. J. R. Gavaler, *Appl. Phys. Lett.*, **23**, 480 (1973).
2. L. R. Testardi, J. H. Wernick, and W. A. Royer, *Solid State Comm.*, **15**, 1 (1974).
3. O. Fischer, H. Jones, G. Bongio, M. Sergent, and R. Chevrel, *J. Phys.*, **C7**, L450 (1974).
4. J. Bardeen, L. N. Cooper, and J. R. Schrieffer, *Phys. Rev.*, **108**, 1175 (1957).
5. W. L. McMillan, *Phys. Rev.*, **167**, 331 (1968).
6. G. W. Cullen, 1968 Summer Study on Superconducting Devices and Accelerators, BNL, p. 437.
7. Proc. of the International Discussion Meeting on Radiation Effects on Superconductivity, 13-16 June 1977 at Argonne, *J. Nuclear Materials*, **72** (1978).
8. O. Meyer, *New Uses of Ion Accelerators*, ed., J. F. Ziegler, Plenum Press, N.Y. (1975).
9. G. Heim and B. Stritzker, *Appl. Phys.*, **7**, 239 (1975).
10. W. Buckel and R. Hilsch, *Z. Physik*, **138**, 109 (1954).
11. W. Buckel, *Symposium of the Electric and Magnetic Properties of Thin Metal Levels*, (Leuven, 1961), p. 264.
12. G. Bergmann, *Phys. Reports*, **27c**, 159 (1976).
13. G. V. Minnigerode and J. Rothenberg, *Z. Physik*, **213**, 397 (1968).
14. A. Fontaine and F. Meunier, *Phys. Mat. Kond.*, **14**, 119 (1972).
15. D. Allender, J. Bardeen, *J. Bray*, *Phys. Rev.*, **B7**, 1020 (1973).
16. E. N. Economou and K. L. Ngai, *Solid State Comm.*, **17**, 1155 (1975).
17. A. M. Lamoise, J. Chaumont, F. Meunier, and H. Bernas, *J. Physique Lett.*, **36**, L-271, L-305 (1975).
18. L. Dumoulin, P. Nedellec, J. Chaumont, D. Gilbon, A. M. Lamoise, H. Bernas, *C.R. Acad. Sc. Paris*, **B283**, 285 (1976).
19. A. M. Lamoise, J. Chaumont, F. Lalu, F. Meunier, and H. Bernas, *J. Physique Lett.*, **37**, L-287 (1976).
20. P. Ziemann et al., *Z. Physik*, **B35**, 141 (1979).
21. F. Meunier, P. Pfeuty, A. M. Lamoise, J. Chaumont, H. Bernas, and C. Cohen, *J. Physique Lett.*, **38**, L-435 (1977).
22. B. Stritzker, H. Wühl, *Z. Physik*, **243**, 361 (1971).
23. E. Hang, N. Hedgecock, W. Buckel, *Z. Physik*, **B22**, 237 (1975).
24. B. Stritzker, H. Wühl, *Z. Physik*, **B24**, 367 (1976).
25. M. M. Collver, R. H. Hammond, *Phys. Rev. Lett.*, **30**, 92 (1973).
26. B. Schroeder, W. L. Johnson, C. C. Tsuei, P. Chaudhari, J. F. Craczyk, *AIP Conf. Proc. (UDA)*, **31**, 353 (1976).
27. O. Meyer, H. Mann, E. Phrilingos, *Application of Ion Beams to Metals*, eds., S. T. Picraux, E. P. EerNisse, F. L. Vook, Plenum Press, N.Y. (1974), p. 15.
28. O. Meyer, *Inst. Phys. Conf. Ser. No.*, **28**, 168 (1976).
29. G. Linker, O. Meyer, *Solid State Comm.*, **20**, 695 (1976).
30. G. Linker in Ref. (7).
31. C. Rizzuto, *Rep. Progr. Phys.*, **37**, 147 (1874).
32. J. Geerk, G. Heim, J. Kessler, *Z. Physik*, **242**, 86 (1971).
33. W. Buckel, M. Dietrich, G. Heim, J. Kessler, *Z. Physik*, **245**, 283 (1971).
34. W. Buckel, G. Heim, *Application of Ion Beams to Metals*, eds., S. T. Picraux, E. P. EerNisse, F. L. Vook, Plenum Press, N.Y. (1974), p. 3.
35. W. Bauriedl and G. Heim, *Z. Physik*, **B26**, 29 (1977).
36. G. Chanin, E. A. Lynton, and B. Serin, *Phys. Rev.*, **114**, 719 (1958).
37. D. Markowitz and L. P. Kadanoff, *Phys. Rev.*, **131**, 563 (1963).
38. D. P. Seraphin, C. Chiou, and D. J. Quinn, *Acta Metallurgica*, **9**, 861 (1961).
39. T. Skoskiewicz, *Phys. Stat. Solidi*, (a), **11**, K 123 (1972).
40. B. Stritzker and W. Buckel, *Z. Physik*, **257**, 1 (1972).
41. B. Stritzker and J. Becker, *Phys. Lett.*, **51A**, 147 (1975).
42. A. Eichler, H. Wühl, and B. Stritzker, *Solid State Comm.*, **17**, 213 (1975).
43. W. Buckel and B. Stritzker, *Phys. Lett.*, **43A**, 403 (1973).
44. M. R. Chowdhury, *J. Phys.*, **F4**, 1657 (1974).
45. A. L. Giorgi, E. G. Szklarz, E. K. Stroms, A. L. Bowman, and B. T. Matthias, *Phys. Rev.*, **125**, 837 (1962).
46. J. Geerk and K.-G. Langguth, *Solid State Comm.*, **23**, 83 (1977).
47. K.-G. Langguth, Ph.D. Thesis, Universität Karlsruhe (1977).
48. K. G. Langguth, G. Linker, and J. Geerk, *Ion Beam Surface Layer Analysis*, eds., O. Meyer, G. Linker, F. Käppeler, Plenum Press, p. 273 (1976).
49. J. M. Poate, R. C. Dynes, L. R. Testardi, and R. H. Hammond, *Phys. Rev. Lett.*, **37**, 1308 (1976).
50. O. Meyer, B. Seeber, *Solid State Comm.*, **22**, 603 (1977).
51. J. M. Soeder and B. Stritzker, in Ref. (7).
52. S. I. Tsypkin and R. S. Chudnova, *Soviet Phys. Solid State*, **13**, 2588 (1972).
53. H. C. Freyhardt, A. Taylor, and B. A. Loomis, *Application of Ion Beams to Metals*, eds., S. T. Picraux, E. P. EerNisse, F. L. Vook, Plenum Press, N.Y., p. 47 (1974).
54. H. C. Freyhardt, in Ref. (7).
55. E. Deprez, Y. Bruynseraede, W. Thys, and L. Reynders, *Phys. Lett.*, **46A**, 458 (1974).
56. C. H. Arrington III and B. S. Deaver, Jr., *Appl. Phys. Lett.*, **26**, 204 (1975).
57. E. P. Harris, *IEEE Trans. on Magn. MAG-11*, 785 (1975); E. P. Harris and R. B. Laibowitz, *MAG-13*, 724 (1977).
58. K. K. Likharev and L. A. Yakobson, *Sov. Tech. Phys.*, **20**, 950 (1976).
59. O. Meyer, in Ref. (7), p. 182.

THE SUPERCONDUCTING TRANSITION TEMPERATURE OF NIOBIUM CARBIDE SINGLE CRYSTALS AFTER IMPLANTATION OF LIGHT ELEMENTS

J. GEERK

*Kernforschungszentrum Karlsruhe GmbH Institut für Angewandte Kernphysik I, Postfach 3640,
D-7500 Karlsruhe 1, Federal Republic of Germany.*

(Paper first read at the International Conference on Ion Beam Modification of Materials, September 4-8, 1978, Budapest, Hungary).

INTRODUCTION

Giorgi *et al.*¹ found that the superconducting transition temperature T_c of niobium carbide with sodium chloride structure is very sensitive to deviations of the carbon content from stoichiometry. The maximum carbon content obtainable by conventional methods is 0.98 corresponding to a T_c of 11.1 K. The difficulty in obtaining a completely stoichiometric carbide of niobium is due to the fact, that the formation of the compound has to be carried out at high temperatures (1400-2000°C). So the equilibrium concentration of carbon vacancies, which exponentially depends on temperature can reach high values (2-24%). By implantation of carbon ions the carbon content could be increased resulting in a T_c of 11.8 K.² An obvious consequence of this experiment is to investigate, if by use of the method of ion implantation the deficient carbon can be substituted by other elements. The results of such implantation experiments are described in this contribution.

EXPERIMENTAL

As starting material we used single crystals of $\text{NbC}_{0.89}$ of NaCl structure with a typical size of $15 \times 4 \times 2$ mm and a T_c of 4 K. The single crystals were produced by zone melting of hot pressed NbC powder samples.³

The implantations were carried out at elevated temperatures between 700 and 1000°C. Figure 1 shows the sample holder used for these experiments. The sample is mounted on the cup shaped anode of an electron gun and heated indirectly up to the desired temperature. During implantation the beam current is measured by a monitor electrode which also is used as a beam defining diaphragm. The sample temperature is controlled by a thermocouple and a pyrometer. The pressure in the target chamber during implantation was about 10^{-8} Torr. Implantation energies and fluences were selected to result in homogeneously implanted

surface layers of about 2000 Å thickness with a concentration of 11-12% at. % of implanted ions.

The superconducting transition temperature was determined resistively by a four probe arrangement. In order to detect the highest transition of the implanted surface layer low measuring currents (100 μA) were used. The resulting voltage drop across the bulk sample (10-100 nV) was measured by a lock in amplifier. The instrumentation is described in more detail in.⁴

RESULTS AND DISCUSSION

The first step in these investigations was to find out the optimum (with respect to T_c) implantation temperature. Figure 2 shows T_c versus implantation temperature for P^+ and S^+ implants. T_c seems to saturate at about 900°C. This is also the optimum implantation temperature for C^+ ions.² J. M. Lombaard and O. Meyer⁵ have shown using the backscattering and channeling technique, that at this implantation temperature the radiation damage in the Nb sublattice is already completely annealed. All implantations described in the following have been carried out between 900 and 920°C.

The table shows the T_c results after implantation of niobium carbide with elements from row 2 and 3 of the periodic system including He from row 1. T_c increases continuously from Li (5.7 K) to N (12.8 K) but O, F and Ne do not continue this trend further. A striking fact is the T_c increase found after rare gas implantation with the highest value of $T_c = 9.7$ K for He.

The T_c increase with increasing number of valence electrons from Li to N can only partially be caused by direct changes in the electronic properties of the host metal, as it is unlikely, that rare gases, especially He give electrons to the Fermi

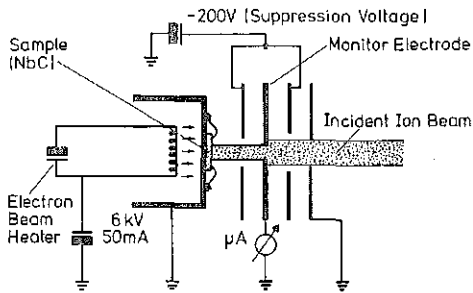
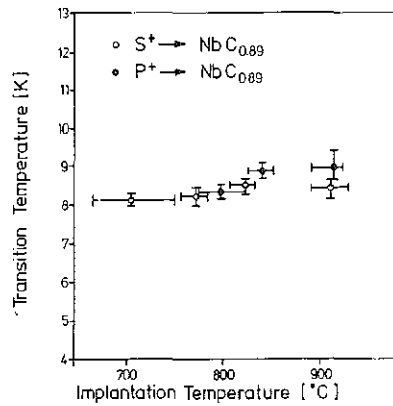


FIGURE 1 Sample holder for hot implantation.

sea. Possibly most of the T_c increase after implantation of light elements is caused just by occupancy of the carbon vacancies by the implanted ion, resulting in a rearrangement of the Nb sublattice.

REFERENCES

1. A. L. Giorgi, E. G. Szklarz, E. K. Storms, A. L. Bowman, and B. T. Matthias, *Phys. Rev.*, **125**, 837 (1962).
2. J. Geerk and K.-G. Langguth, *Solid State Commun.*, **23**, 83 (1977).
3. B. Scheerer and W. Reichardt, *Progress Report of the Teilinstitut Nukleare Festkörperphysik*, Ges. f. Kernforschung mbH, Karlsruhe (KFK 2357), 74 (1974).
4. K.-G. Langguth and J. Geerk, *Progress Report of the Teilinstitut Nukleare Festkörperphysik*, Ges. f. Kernforschung mbH, Karlsruhe (KFK 2054), 104 (1976).
5. J. M. Lombaard and O. Meyer, *Rad. Eff.*, **36**, 83 (1977).

FIGURE 2 The transition temperature of $\text{NbC}_{0.89}$ single crystals as a function of implantation temperature for S^+ and P^+ implantation.

Element	He	Li	Be	B	C	N	O	F	Ne	P	S	Ar
VE	(2)	1	2	3	4	5	6	7	(8)	5	6	(8)
T_c	9.7	5.7	8.5	10.2	11.8	12.8	9.5	10.0	9.3	8.8	8.4	8.0

SUPERCONDUCTING PROPERTIES AND STRUCTURE OF ION BOMBARDED Nb LAYERS

G. LINKER

*Kernforschungszentrum Karlsruhe GmbH Institut für Angewandte Kernphysik I, Postfach 3640,
D-7500 Karlsruhe 1, Federal Republic of Germany.*

(Paper first read at the International Conference on Ion Beam Modification of Materials, September 4-8, 1978, Budapest, Hungary).

The influence of ion bombardment on the superconducting transition temperature T_c and the structure of thin evaporated niobium layers has been investigated as a function of ion species and layer purity. Irradiation through pure layers with neon ions and fluences of typically 10^{16} ions/cm² leads to relatively small T_c decreases ($\Delta T_c \sim 0.5$ K), while in oxygen contaminated layers larger effects depending on oxygen concentration are observed. Homogeneous implantation of chemically active impurities (nitrogen, oxygen) also drastically depresses T_c , reaching the detection limit of 1.2 K at a concentration of 15 at. % N. The T_c depressions correlate with a lattice parameter expansion of the Nb bcc structure at a rate of about 0.1 % per 1 at. % impurity.

INTRODUCTION

Niobium is under normal conditions the elemental superconductor with the highest superconducting transition temperature T_c of 9.3 K. T_c in niobium is sensitive to disorder and to interstitially dissolved impurities. Substantial depressions of T_c , e.g. were observed in bulk samples with a few at. % dissolved oxygen,^{1,2} or in layers where a high degree of disorder was introduced by vapor deposition onto cryogenic substrates.^{3,4} The influence of impurities on the stabilization of disordered phases of quench condensed Mo and Nb layers has recently been shown by Schroeder *et al.*⁵ Both disorder and impurities may be conveniently introduced into thin metal films in a quantitative way by ion bombardment.

The influence of ion implantation and of irradiation through the layers with the bombarding particles being stopped in the substrates on the superconducting transition temperature has been already studied in molybdenum and vanadium thin films.^{6,7} Substantial changes of T_c have been observed in these experiments with T_c of Mo increasing up to 9.2 K and T_c of V decreasing down to the detection limit of 1.2 K. The T_c alterations were a function of the impurity concentration and were depending on ion species. T_c was affected strongly by the implantation or activation (i.e. for example recoil implantation from oxide precipitates) of chemically active im-

purities like oxygen or nitrogen while layer bombardment with Ne ions caused only smaller effects.

In this contribution the influence of ion doping and disorder produced by the irradiation process on T_c and the structure of evaporated niobium films has been studied. The questions whether the T_c variations are correlated with structural distortions and whether disorder is stabilized by chemically active impurities were of special interest.

EXPERIMENTAL PROCEDURE

Niobium thin films with thicknesses in the range of 120-250 nm were prepared by electron beam evaporation onto quartz and vitreous carbon substrates kept at room temperature or heated to 500-800°C. The background pressure in the chamber typically was 2×10^{-9} Torr, and rose during deposition to about 5×10^{-8} Torr at evaporation rates of 3 nm/s. Some layers were deposited under reactive gas atmosphere (oxygen, nitrogen) with partial pressures varied in the range from 5×10^{-8} to 1×10^{-5} Torr.

Film thickness, purity, homogeneity and the impurity content and distribution have been analysed using Rutherford backscattering of 2 MeV He ions. The analysis of the films deposited onto the carbon substrates allowed a concentration determination of oxygen and nitrogen down to about 0.5 at. %.

Ion bombardment was performed at room temperature with oxygen, nitrogen and neon ions. A homogeneous doping of the layers was performed by multiple energy implantation with fluences obtained from calculated implantation profiles. An example of a calculated profile is demonstrated in Figure 1. The implantations were performed with fluences corresponding

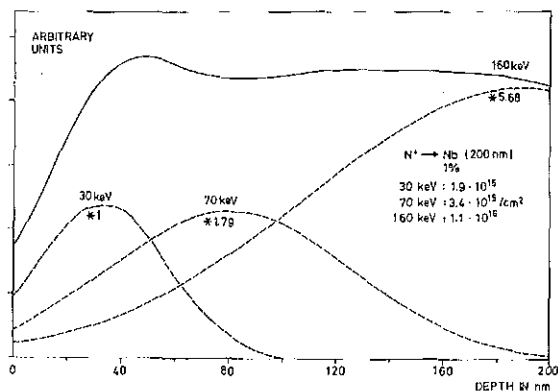


FIGURE 1 Calculated implantation profile for nitrogen in a 200 nm thick niobium layer. Energy values and fluences for a 1 at. % doping are indicated in the figure.

to concentration values in the range from 1 to 30 at. %. "Pure" damage in the layers was created by 360 KeV Ne ion bombardment, such that the ions penetrated the layers and stopped in the substrates (layer irradiation). With this procedure a rather homogeneous primary energy deposition is achieved in layers with thicknesses of about 150 nm. Fluences in the range of 1×10^{15} – 1×10^{17} ions/cm² were used in the irradiation experiments.

A thin film Guinier-camera was employed for X-ray analysis supplying structural informations like the phase, the lattice parameter and the grain size in the layers.

The transition temperature was measured resistively using a standard four-probe arrangement. The resistivity and the resistance ratio r ($r = R_{300}/R_{10}$) of the layers were also determined and considered as a measure of layer quality and defect concentration in as evaporated and in ion bombarded layers, respectively. The lowest temperature obtainable in our cryostat was 1.2 K.

RESULTS AND DISCUSSION

The properties of the as evaporated Nb layers were depending on the deposition conditions. Layers prepared under optimum vacuum conditions onto substrates at room temperature had T_c -values around 9.4 K and r -values of about 4. The oxygen content determined from layers on carbon substrates was in the range between 1–2 at. %. Layers prepared at elevated substrate temperatures (500–600°C) had T_c values of 9.3 K, r values up to 10 and oxygen contents below 1 at. %. The high T_c -values in layers with relatively high oxygen contents indicate that oxygen was not interstitially incorporated into the Nb bcc-structure but probably was present in the layers in form of oxide precipitates at grain boundaries.¹ At substrate temperatures above 700°C both T_c and r decreased. Similarly evaporations in oxygen or

nitrogen atmospheres led to enhanced impurity contents in the layers and to reductions of T_c down to the detection limit and of r values below 1 depending on the partial reactive gas pressure in the evaporation chamber.

All the layers evaporated under optimum vacuum conditions revealed the pure bcc-structure. The determination of the lattice parameter was not unique due to strain in the layers. Therefore a procedure on a relative scale taking a mean value of the lattice parameter determined from the (310), (222) and (321) lines was adopted. These lines are closest to the diffraction angle $\theta = 55^\circ$ where the internal strain vanishes.⁸ This procedure yielded a lattice parameter of 3.301 which is close to the bulk value of 3.3006. A considerable difference in line width was observed for layers prepared at room temperature and at elevated temperatures. Particle sizes of about 12 nm and of 25 nm have been estimated for the different temperatures respectively if the line broadening was ascribed to particle size effects alone. Evaporation in the presence of reactive gases resulted in distortions of the Nb bcc-structure with considerable line broadening, intensity decrease and a line shift to lower angles indicating a lattice parameter increase. The degree of distortion was depending on impurity content and an amorphization of the layers was observed at about 30 at. % of impurities incorporated into the layers.

The results of the analysis of the as evaporated layers show that r -values closely correlate with growth conditions (substrate temperature). Small oxygen contents probably present in the layers in form of oxide precipitates do not affect T_c . Both r and T_c however are sensitive to impurities incorporated into the bcc-structure and are strongly affected via grain size effects at high impurity levels finally causing amorphization of the structure.

The ion bombardment of the Nb layers resulted in decreases of the transition temperature T_c , reductions of the resistivity ratio r and in structural distortions. These effects were depending on ion species and layer purity.

Implantations with nitrogen, oxygen and neon ions were performed into layers with the least oxygen content. A homogeneous doping is essential when T_c decreases have to be detected. The homogeneity of the implantation performed with the procedure described above was tested by the backscattering technique. As an example backscattering peaks from an unimplanted and an im-

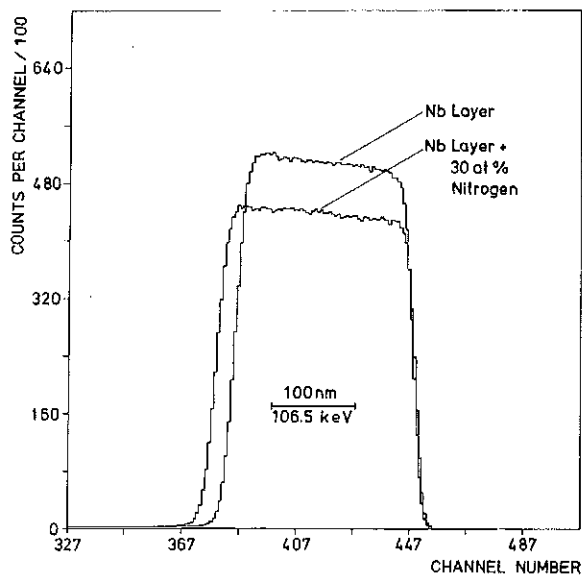


FIGURE 2 Niobium peaks from backscattering spectra of a layer before and after implantation with a high dose nitrogen indicating a homogeneous impurity distribution.

planted (with 30 at.% N) area on a Nb layer are shown in Figure 2. The reduced peak height in the spectrum from the implanted layer is due to the change of the energy loss on account of the incorporated nitrogen thus reflecting the nitrogen distribution. The peak areas are proportional to the number of the Nb atoms. The relatively small decrease of the peak area ($\sim 3\%$) after the high fluence bombardment necessary for a 30 at.% doping indicates that sputtering effects are small in the implantation experiments.

The influence of nitrogen implantation on T_c is shown in Figure 3 where T_c of the implanted layers is plotted versus nitrogen concentration determined from the implantation fluences. Different T_c values, at the same concentration indicate the reproducibility of the experiments performed with different layers. A continuous depression of T_c is observed with nitrogen concentration down to the T_c detection limit at 15 at.% N. For higher N concentrations a slight T_c increase is observed. Though this effect must be still confirmed it may be due to nitride precipitation in the layers. An increase of T_c after a high dose nitrogen implantation into Nb layers above the initial value together with probable δ -NbN formation after annealing was reported by Gamo *et al.*⁹ These authors also observed a peak formation in the range of implanted nitrogen in channelling-backscattering

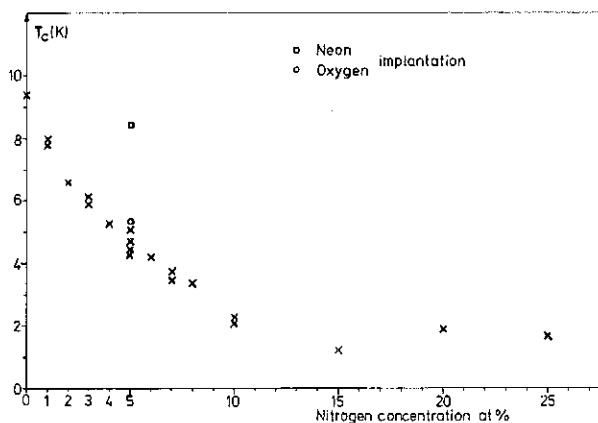


FIGURE 3 T_c as a function of implanted nitrogen concentration. T_c -values for 5 at.% oxygen and neon implantation are included for comparison.

experiments with implanted Nb single crystals. These results agree with our own observations where peak formation starting at about 20 at.% N concentration was detected indicating phase transformations.¹⁰

In addition to the nitrogen implantations oxygen and neon profiles corresponding to 5 at.% impurity concentration were implanted for comparison. While oxygen caused a similar T_c depression like that observed for nitrogen only a relatively small effect occurred for the neon implantation. The measurement points are included in Figure 3.

In the irradiation experiments with Ne ions through the layers T_c depressions have also been observed. Here the effect was a function of ion fluence and was depending on oxygen content. Results for two layers, NbE 921 and NbE 1032, with oxygen contents of less 0.5 at.% and of 7.4 at.% and initial T_c values of 9.18 K and 8.13 K, respectively, irradiated with fluences of 1×10^{16} , 5×10^{16} and 1×10^{17} Ne^+/cm^2 are quoted here as an example. The relative T_c depressions, $\Delta T_c/T_c$, for the three fluences were for NbE 921: 0.057, 0.14, 0.25 and for NbE 1032: 0.12, 0.26, 0.51, respectively. This example shows that the larger T_c depressions occur in layers with the higher oxygen content in accordance with similar observation in vanadium layers.⁷ The effect is thought to be due to impurity activation during the irradiation process, i.e. recoil implantation of oxygen into the Nb grains from oxide precipitates or surface oxide layers. Thus the quantitative results will depend on grain size; this and also the role of surface oxides must still be explored in detail to quote quantitative results.

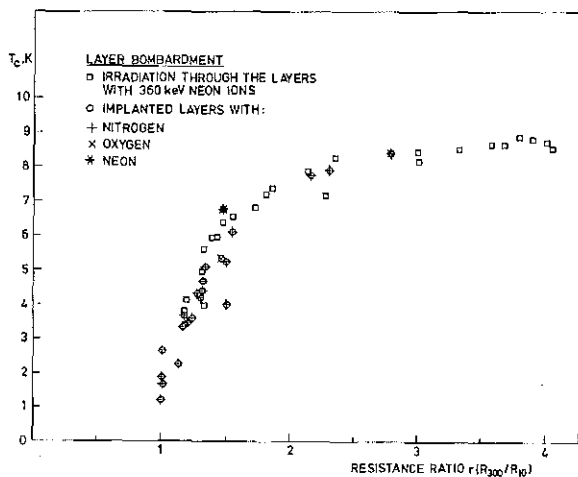


FIGURE 4 T_c of irradiated and implanted Nb layers as a function of the resistance ratio r .

The T_c depressions in the implanted and irradiated layers were accompanied by a decrease of the resistance ratio r , and a correlation between T_c and r in a rather narrow band was found. This T_c versus r relationship is plotted in Figure 4, showing T_c saturation for r -values above 3 and a sharp drop for r -values below 2. The unique relationship between T_c and r irrespective of the irradiation and implantation conditions and the initial properties of the Nb layers suggests a common defect structure in the ion bombarded layers. A similar relationship in as prepared and ion irradiated Nb-Ge superconducting films has been already reported by Poate *et al.*¹¹

X-ray analysis of the bombarded layers revealed that the T_c depressions correlate with distortions of the Nb bcc-structure. The bcc-structure is preserved up to an impurity concentration of 15 at.% showing some line weakening and a considerable increase of the lattice parameter a . The relative change of a is shown in Figure 5 as a function of nitrogen concentration with an almost linear increase up to 20 at.% N. In the nitrogen concentration range of 20–25 at.% the high angle lines disappeared and only faint and broad low angle lines were observed indicating heavy structural distortions towards amorphization. At 30

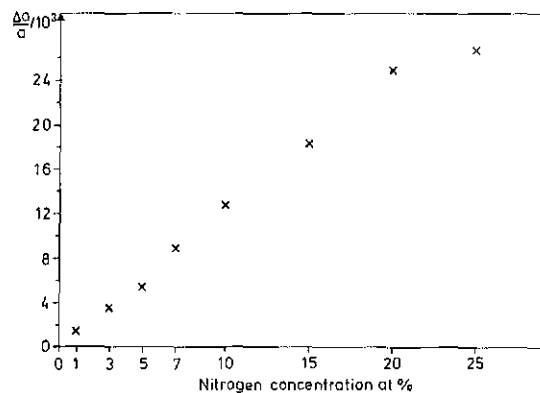


FIGURE 5 The relative increase of the lattice parameter in implanted Nb layers as a function of nitrogen concentration.

at.% new lines appear in the X-ray photographs probably due to nitride precipitation as discussed before.

In summary, T_c in niobium layers is sensitive to implanted or activated chemically active impurities causing depression down to 1.2 K. A common defect structure is suggested to be responsible for this effect. X-ray analysis showed that the impurities cause a distortion of the bcc phase with a sizable lattice expansion and with the degree of distortion growing with impurity concentration.

REFERENCES

1. W. DeSorbo, *Phys. Rev.*, **132**, 107 (1963).
2. C. C. Koch, J. O. Scarbrough, D. M. Kroeger, *Phys. Rev.*, **B9**, 888 (1974).
3. J. E. Crow, M. Strongin, R. S. Thompson, and O. F. Kammerer, *Phys. Lett.*, **A30**, 161 (1969).
4. M. M. Collver, R. H. Hammond, *Phys. Rev. Lett.*, **30**, 92 (1973).
5. B. Schroeder, W. L. Johnson, C. C. Tsuei, P. Chaudhari, and J. E. Graczyk, *AIP Conf. Proc. (USA)*, **31**, 353 (1976).
6. G. Linker and O. Meyer, *Sol. State Comm.*, **20**, 695 (1976).
7. G. Linker, *J. Nucl. Mat.*, **72**, 275 (1978).
8. R. Feder, B. S. Berry, *J. Appl. Cryst.*, **3**, 372 (1970).
9. K. Gamo, H. Goshi, M. Takai, M. Iwaki, K. Masuda, S. Namba, *J. J. Appl. Phys.*, **16**, 1853 (1977).
10. T. Hussain, G. Linker, unpublished results.
11. J. M. Poate, L. R. Testardi, A. R. Storm, and W. M. Augustyniak, *Inst. Phys. Conf. Ser. No.*, **28**, 176 (1976).

X-RAY DIFFRACTION STUDIES ON He- AND Ar-IRRADIATED Nb₃Ge THIN FILMS

J. Pflüger and O. Meyer

Kernforschungszentrum Karlsruhe, Institut für Angewandte Kernphysik, P.O. Box 3640, D-7500 Karlsruhe,
Federal Republic of Germany

(Received 16 July 1979; in revised form 30 July 1979 by P.H. Dedrichs)

We have performed measurements of relative integrated X-ray intensities in order to study the influence of radiation damage on the A15 structure of superconducting Nb₃Ge. With increasing He- and Ar-ion fluence an increase of the "temperature factor" and the lattice parameter has been observed in the fluence region where the depression of the superconducting transition temperature T_c was found to occur. Both parameters do not uniquely depend on the decrease of T_c . Further a decrease of the total relative X-ray intensity is found for particle fluences in the saturation region of T_c . The results are interpreted in terms of static atom displacements statistically distributed in the irradiated volume.

1. INTRODUCTION

THE SUPERCONDUCTING transition temperature of material with A15 structure is strongly depressed by particle and neutron irradiation [1–4]. The nature of defects responsible for this decrease is still uncertain. Three kinds of defects structures have been identified up to now. (1) Disordered microregions observed with small-angle neutron scattering [5] and transmission-electron-microscopy [6] in neutron irradiated Nb₃Sn. (2) Antisite defects, i.e. the interchange of A- and B-atoms from X-ray and neutron diffraction experiments after irradiation with fast neutrons [7]. (3) Static displacements of atoms from their ideal lattice sites by channeling experiments on He- and Kr-irradiated V₃Si-single crystals [2, 8, 9]. From similarities in the dependence of various physical properties such as electrical resistivity, specific heat, magnetic susceptibility and upper critical field on irradiation with different particles such as electrons or light ions and heavy ions or neutrons, which are known to produce quite different damage structures, the existence of a universal defect preferentially responsible for the observed changes have been suggested [3]. It has been shown earlier that different damage structures are present in V₃Si-single crystals after irradiation with light (He) and heavy (Kr) noble gas ions [2, 10]. In strongly disordered regions produced after Kr-irradiation the distribution of displaced lattice atoms was also found to be inhomogeneous with a normal distribution around their original lattice site. The average displacement amplitude was found to increase with increasing Kr-ion fluence up to a fluence of about 4×10^{14} Kr cm⁻², where a complete amorphisation was reached [13].

In order to get more information on the existence

of static displacements in polycrystalline material with A15 structure after irradiation with light and heavy ions we performed measurements of relative integrated X-ray intensities on superconducting Nb₃Ge-layers before and after irradiation with 350 keV He- and 650 keV Ar-ions.

2. EXPERIMENTAL

Nb₃Ge layers, about 220 to 250 nm thick have been produced by simultaneous evaporation onto hot sapphire substrates (~ 850°C). Layers were irradiated at room-temperature with various fluences of 300 keV He- and 650 keV Ar-ions. The energies chosen allowed the ions to penetrate through the Nb₃Ge layers and come to rest in the substrates. Critical temperatures and resistivities were determined by using a standard four-point probe technique. Lattice parameter and intensity measurements were carried out with a Seemann–Bohlin focusing camera and a Seemann–Bohlin focusing diffractometer. A Ge-monochromator was used to select Cu-K_{α1}-radiation.

In order to provide a reproducible installation in the diffractometer as well as in the ion-irradiation and T_c -measuring facilities, the samples were mounted on special sample holders. In this way measurements were performed on exactly the same spot. The area irradiated with ions was larger (about 10 mm in diameter) than the X-ray beam diameter (about 3 × 5 mm). Intensities of 13 lines from the Nb₃Ge layer were measured prior and after irradiation at different fluences. In order to cancel out long time drift on the X-ray tube, the integrated 311 line of a gold layer was routinely used to calibrate the intensities on a relative scale. The results are plotted as the natural logarithm of the X-ray intensity ratio I/I_0 vs $(\sin^2\theta)/\lambda^2$ where λ denotes the wavelength of the X-ray

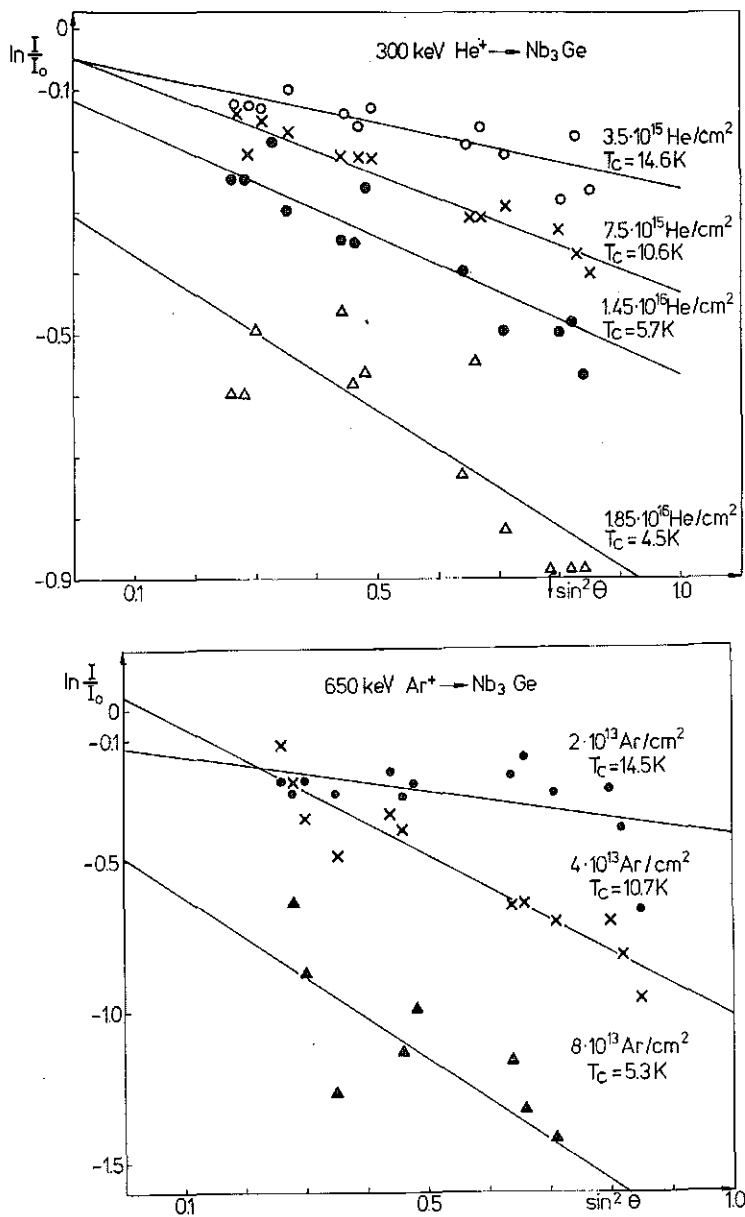


Fig. 1. (a) The natural logarithm of the integrated X-ray intensity ratio I/I_0 as a function of $\sin^2 \theta$. The X-ray intensity I as measured after He-irradiation with various fluences indicated in the figure is normalized by I_0 , the intensity prior to irradiation. (b) Similar functional dependence as in (a) after irradiation with various Ar-fluences as indicated in the figure.

radiation employed. I is the intensity of a particular line after irradiation and I_0 the intensity of the same reflex prior to irradiation. The intensity ratio is altered due to irradiation effects only. The lattice parameters were determined at an angle of 45° to the substrate surface where it has been shown that the influence of stress effects will cancel out [11].

3. RESULTS

Single phase A15 Nb₃Ge layers have been produced with T_c -values of 21.7 K at half transition and with a

transition width of about 1 K. Residual resistivity ratio values up to 2 were reached and the lowest residual resistivity value was $40 \mu\Omega\text{-cm}$. Lattice parameters measured for these layers were 5.145 \AA .

The natural logarithm of the integrated intensities ratio is presented in Figs. 1(a) and (b) as function of $\sin^2 \theta$ after irradiation with various fluences of He- and Ar-ions. The fluences and the superconducting transition temperatures determined after irradiation are indicated in Figs. 1(a) and (b). Least square fit straight lines have been drawn through the experimental points. The slope

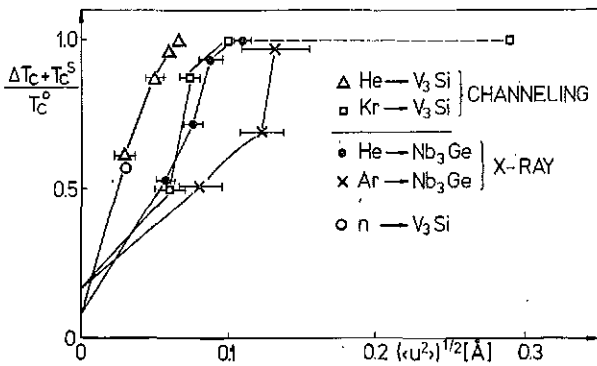


Fig. 2. The relative decrease of T_c after irradiation with He- and Ar-ions as function of the average displacement amplitude. Results obtained from channeling measurements on He- and Ar-irradiated V₃Si-single crystals are included for comparison. Further included is the result of a neutron diffraction experiment on a neutron irradiated V₃Si-single crystal [12].

of these curves is equal to $2B/\lambda^2$, where B , the temperature coefficient, is equal to $8\pi^2\langle u_1^2 \rangle$ and $\langle u_1^2 \rangle$ is the mean square displacement of atoms from their mean position normal to the reflecting plane. No discrimination has been made between Nb- and Ge-atoms. With increasing ion fluence and decreasing T_c the slope and therefore $\langle u_1^2 \rangle$ is found to increase for He – as well as for Ar – irradiated layers. A similar saturation value T_c^s of T_c equal to 3.8 K is observed for He – as well as for Ar – irradiation to high fluences.

Besides the intensity loss due to an increase in the temperature factor there is a loss of total intensity at high ion fluences, i.e. the intensity of all lines decreased by the same amount. This is indicated by the points of intersection of the straight lines with the ordinates in Figs. 1(a) and (b). The total intensity loss increases

strongly in the fluence region where T_c -saturation occurs. For He-fluences where T_c is lowered to 5.7 and 4.5 K the total intensity loss is $7 \pm 2\%$ and $25 \pm 8\%$, respectively. If T_c is lowered to 5.3 K by Ar-irradiation the total intensity loss is even $40 \pm 12\%$. At Ar-fluences of about 2×10^{14} Ar cm⁻² causing a T_c -reduction to the saturation of 3.8 K, reflexes could no longer be separated from the background indicating that the layer is nearly amorphous.

The dependence of the relative T_c -reduction $(\Delta T_c + T_c^s)/T_c^0$, where ΔT_c is equal to $T_c^0 - T_c^{irr}$ with T_c^{irr} being the T_c -values for the non-irradiated and the irradiated layer respectively, on the mean square displacement is shown in Fig. 2. For equal values of reduced T_c , $(\langle u_1^2 \rangle)^{1/2}$ -values are larger for Ar- than for He-irradiated layers. For the He-irradiated layer a complete T_c -reduction corresponds to a mean displacement amplitude of 0.1 Å. Static displacements seem to be a common defect in irradiated A15 materials as it has also been observed for He-irradiated V₃Si single crystals using the channeling technique [8–10]. The values for He- and Kr-irradiated V₃Si-single crystals as measured by the channeling technique have been included in Fig. 2. The displacement amplitudes measured after Kr-irradiation are larger than those of He-irradiated V₃Si-single crystals and continue to increase at large fluences in the region of T_c -saturation. Also included in Fig. 2 is the mean displacement amplitude as measured by Cox and Tarvin [12] for a neutron irradiated V₃Si-single crystal in good agreement with the channeling data.

For similar values of reduced T_c the relative integrated X-ray intensity is smaller for Ar-irradiated layers than that for the He-irradiated Nb₃Ge-layers. This is clearly visible in Fig. 3 where T_c is plotted in dependence of $\ln(I/I_0)$ for the 521-line. This difference in intensity

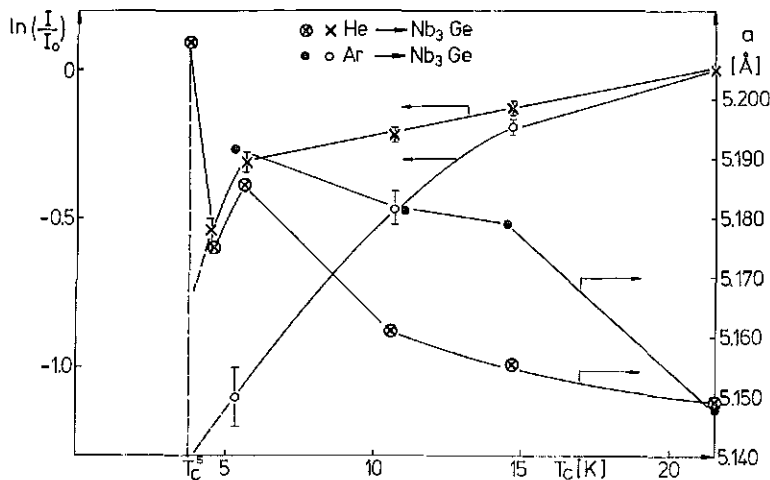


Fig. 3. Natural logarithm of the X-ray integrated intensity ratio of the 521 reflex and the lattice parameter as a function of T_c after irradiation of Nb₃Ge-layers with He- and Ar-ions.

is partly due to the enhanced average displacement amplitude for Ar-irradiated Nb₃Ge-films. In addition an increasing amount of total intensity loss is observed for Ar-irradiated samples with T_c -values below 10 K. The reduction of intensity is caused by the enhanced production of disordered regions in the collision cascade of the Ar-ions. The increased damage level in Ar-irradiated samples obviously does not influence T_c as it is not present in He-irradiated Nb₃Ge-layers.

The lattice parameter of the irradiated samples as function of Ar- and He-fluence is also shown in Fig. 3. The increase of the lattice parameter with increasing fluence and decreasing T_c -values is stronger for Ar-irradiated than for the He-irradiated samples indicating that the lattice parameter does not uniquely depend on T_c however does depend on the amount of damage produced in irradiation experiments.

4. SUMMARY AND DISCUSSION

We have observed that for similar reduced T_c -values the increase of the lattice parameter, the mean displacement amplitude and the amount of randomly displaced atoms (total loss of X-ray intensity) is larger for Ar- than for He-irradiated Nb₃Ge-layers. With increasing He- and Ar-ion fluences the differences in lattice parameter, mean displacement amplitude and amorphous component increase and a total amorphisation of the irradiated volume is reached for a fluence of 2×10^{14} Ar cm⁻².

These observations are in agreement with results obtained from channeling experiments on He- and Ar-irradiated V₃Si single crystals, where two different damage components have been seen: (a) the first component, preferentially produced after He-irradiation in the transmission region of the He-particles, consisted of statistically displaced V-atoms from their lattice site with a comparatively small average displacement amplitude of 0.05 Å. The second damage component which is preferentially produced at the end of the He-track or along the total track of heavy ions was inhomogeneously distributed in the irradiated volume. This second damage component as produced in the collision cascades consisted of displaced V-atoms having a normal distribution around their original lattice site and an amorphous component. The channeling results indicate that V-atoms are displaced with a large mean displacement amplitude, for example 50 at.% V-atoms with 0.5 Å [10, 13].

The strong increase of the mean displacement amplitude in Ar-irradiated Nb₃Ge-layers is probably due to this second damage component, which completely shadows the possible existence of the first component. A continuous transition between increasing displacement amplitude to a random distribution of atoms is observed during irradiation indicating that the atoms have stable positions in any distance from their original lattice sites.

T_c does not directly depend on the temperature factor and the lattice parameter. The lattice parameter however seems to depend on the amount and structure of the damage present. For the discussion of a possible dependence between damage and T_c the distribution of the damage in the irradiated volume is most important. The displacement of nearly all Nb-atoms with an average displacement amplitude of about 0.1 Å as observed for He irradiated Nb₃Ge-layers is sufficient to lower T_c to its saturation value. This displacement amplitude is about twice as large as that observed for He-irradiated V₃Si. The second damage component, large displacement amplitudes of less lattice atoms, is not present after He-irradiation up to moderate fluences and does therefore not contribute to the T_c -reduction mechanism. In Ar-irradiated Nb₃Ge-layers this second damage component determines the temperature factor and the lattice parameter and shadows therefore the possible existence of the first damage component. Here we have only indirect hints such as the functional dependence of T_c on the residual resistivity, ρ_0 , which is similar for He- and Ar-irradiation and from a similar functional dependence of ρ_0 on the He- and Ar-fluence indicating that the first damage component exists as well after heavy ion irradiation and is responsible for the T_c -reduction mechanism.

The accuracy of the present X-ray intensity measurements does not allow to evaluate the possible influence of anti-site defects as a source for the T_c -reduction mechanism, especially as the scattering powers of Nb and Ge are not very different.

REFERENCES

1. A.R. Sweedler, D.E. Cox & S. Moehlecke, *J. Nucl. Mater.* **72**, 50 (1978).
2. O. Meyer, *J. Nucl. Mater.* **72**, 182 (1978).
3. L.R. Testardi, J.M. Poate & H.J. Levinstein, *Phys. Rev.* **B15**, 2570 (1977).
4. B. Besslein, G. Ischenko, S. Klaumünzer, P. Mueller, H. Neumüller, K. Schmelz & H. Adrian, *Phys. Lett.* **53A**, 49 (1975).
5. A.E. Karkin, V.E. Arkhipov, B.N. Goshchitskii, E.P. Romanov & S.K. Sidorov, *Phys. Status Solidi (a)* **38**, 433 (1976).
6. C.S. Pande, *Solid State Commun.* **24**, 241 (1977).
7. A.R. Sweedler & D.E. Cox, *Phys. Rev.* **B12**, 147 (1975).
8. O. Meyer & B. Seeber, *Solid State Commun.* **22**, 603 (1977).
9. L.R. Testardi, J.M. Poate, W. Weber, W.M. Angustyniak & J.H. Barrett, *Phys. Rev. Lett.* **39**, 716 (1977).
10. R. Kaufmann & O. Meyer, *Rad. Effects* **40**, 161 (1979).
11. R. Feder & B.S. Berry, *J. Appl. Crystallogr.* **3**, 372 (1970).
12. D.E. Cox & J.A. Tarvin, *Phys. Rev.* **B18**, 22 (1978).
13. G. Linker, R. Kaufmann & O. Meyer (unpublished results).

The Influence of Light- and Heavy-Ion Irradiation on the Structure, Resistivity, and Superconducting Transition Temperature of V_3Si . A Comparative Study

O. Meyer and G. Linker

Kernforschungszentrum Karlsruhe GmbH, Institut für Angewandte Kernphysik,
Karlsruhe, West Germany

(Received September 4, 1979)

Channeling and x-ray diffraction measurements on Kr- and He-irradiated V_3Si single crystals and films reveal different damage levels for fluences in cases where the superconducting transition temperature T_c has been reduced by the same amount. This indicates that only special defect structures are responsible for the T_c -reduction mechanism. In the fluence region where T_c is decreasing, T_c correlates with residual resistivity ρ_0 , independent of the kind of irradiation. However, at particle fluences where T_c saturation occurs, different saturation values of ρ_0 are observed. The exponential decrease and the saturation of T_c with fluence are explained by a similar behavior of ρ_0 versus fluence in the damage production and saturation processes. The increase of the lattice parameter is not uniquely dependent on the decrease of T_c , but also on the amount of damage present.

1. INTRODUCTION

Numerous studies have been performed on the influence of irradiation on the physical properties of superconducting materials with the A-15 structure (see, e.g., Ref. 1). Large depressions of the superconducting transition temperature T_c have been observed after irradiation with neutrons,² heavy ions,^{3,4} light ions,⁵ and electrons.⁶ Different defect structures and defect density distributions are produced during irradiation with electrons or light ions and neutrons or heavy ions. Nevertheless, the mechanism responsible for the radiation-induced reduction of T_c appears to be similar. From this, the question arises of whether there exists a universal defect which indeed could ultimately limit the highest T_c value obtainable in materials with the A-15 structure.⁵

Several kinds of defects have been determined in the past: (a) From x-ray diffraction measurements a reduction of the Bragg-Williams long-range order parameter S ,⁷ which is theoretically related to T_c ,⁸ was found. (b) In neutron-irradiated Nb₃Sn disordered regions of sizes between 20 and 60 Å have been observed, surrounded by a less disordered matrix. The proximity effect between these disordered regions with low T_c and the surrounding matrix with high T_c was proposed to explain the exponential decrease of T_c with neutron fluence.⁹ (c) In irradiated V₃Si single crystals the existence of static atomic displacements has been determined.^{10,11} Monte Carlo computer simulations of these channeling measurements confirmed the defect model of statistically distributed static displacements.¹² As a consequence of this damage, the symmetry of the system is disturbed, which may effect the electronic properties of the material.

A controversial discussion arose at the International Discussion Meeting on Radiation Effects on Superconductivity at Argonne¹ and afterwards¹³ on the existence of different T_c degradation mechanisms in light-ion and neutron-irradiated A-15 materials. In this paper a comparative study has been performed on V₃Si thin films and V₃Si single crystals irradiated with light ions (He) and heavy ions (Kr) in order to determine similarities or dissimilarities in the correlations between T_c and fluence, electrical resistivity, x-ray intensity, lattice parameter, and dechanneling cross section. The results, we hope, will lead to a better understanding of the defect structures present after irradiation with ions transferring quite different mean energies in primary collisions to the lattice atoms, and on the influence of these defect structures on the various physical properties mentioned above.

2. EXPERIMENTAL

A HF sputtering system was used for the preparation of V₃Si thin films. The geometry of the composed V and Si cathode was optimized in order to get laterally homogeneous layers with a 3/1 ratio for V/Si over a length of 3 cm. The following parameters were used during deposition: HF power 300 W, bias voltage 1300 V, Ar pressure 1.3×10^{-1} Torr. None of these parameters had a strong influence on the growth process and film properties. Single-crystalline V₃Si films were deposited on hot, single-crystalline Al₂O₃ substrates. The substrate temperature was found to be the most important parameter for epitaxial growth. Polycrystalline films for x-ray analysis were deposited on slightly lapped Al₂O₃ substrates. Composition, thickness, and the degree of crystallinity have been determined by using 2-MeV He-ion backscattering and channeling.¹⁴ The layers have been irradiated at room temperature with 350-keV He ions or 600-keV Kr ions. Similar irradiations

have been performed with a V_3Si single crystal cut perpendicular to the $\langle 110 \rangle$ direction.

Structural information has been obtained by diffraction measurements employing a thin-film x-ray camera and a thin-film diffractometer. The resistivity and the superconducting transition temperature were determined resistively using a standard four-point probe arrangement. The lowest temperature attainable in our cryostat was 1.2 K. Isochronal annealing has been performed in vacua of 10^{-7} Torr up to $700^\circ C$ and of 10^{-9} Torr for higher temperatures.

3. DEFECT PRODUCTION PARAMETERS

The mean projected range R_D of 350-keV He and 600-keV Kr ions in V_3Si is about 920 nm for He and 110 nm for Kr. With these energies the particles penetrated the V_3Si layers, which had a thickness of 200 nm for He and 50 nm for Kr irradiation. The energy density deposition profiles of the bombarding ions have been calculated by a computer program of Brice.¹⁵ For He particles the energy loss due to nuclear collisions is nearly independent of the depth within the film thickness (transmission region) and is found to be 2.3 eV/nm. For Kr ions the energy density deposited into nuclear collisions increases as a function of depth. The energy loss is 500 eV/nm at the surface and is about 1400 eV/nm at a depth of 50 nm.

In order to estimate the cross section for primary collisions σ_D , the mean energy transferred in such a collision \bar{T} , and the mean free path of the bombarding ion l_{PK} , a Nielsen potential has been used.¹⁶ In Table I the calculated values are summarized for 350-keV He and 600-keV Kr ions and are compared with data for neutron irradiation in a reactor.

Due to the energy distribution of neutrons in a reactor there also results a distribution of \bar{T} ranging from 5 keV for a neutron with 100 keV to 100 keV for a neutron with 2 MeV. At low neutron energies, \bar{T} is similar to the value for Kr-ion irradiation; for high neutron energies the primary

TABLE I

Comparison of Damage Production Parameters for 350-keV He, 600-keV Kr, and 0.1–2-MeV n in V_3Si

	R_D , nm	$(dE/dx)_{\text{nuclear}}$, eV/nm	σ_D , cm^2	\bar{T} , keV	l_{PK} , nm
350-keV He	920	2.3	3.4×10^{-18}	0.2	39
600-keV Kr	110	500–1400	1.2×10^{-16}	4	1.1
0.1–2-MeV n	10^9	—	2.5×10^{-24}	5–100	5×10^7

knocked-on lattice atom can be considered to behave in the defect production like a heavy ion directly implanted at energies of about 100 keV. Thus we expect similar damage structures for Kr- and *n*-irradiated samples, which differ from those produced by He irradiation. As l_{PK} is only 1.1 nm for Kr ions compared to 39 nm for He ions, one expects a higher density of defects along the track of the Kr ions.

4. RESULTS

4.1. Film Quality

The V₃Si films sputtered onto Al₂O₃ single-crystalline substrates were found to be single crystalline with a mosaic spread of 0.6 deg as determined by channeling measurements.¹⁴ The highest T_c value obtained was 16.7 K with a transition width ΔT_c of 0.1 K. The highest residual resistivity ratio r was 22. Polycrystalline V₃Si films had T_c values of 16.4 K with ΔT_c of 0.2 K and r values up to 17. The residual resistivities ρ_0 of these films were found to be between 2.5 and 5 $\mu\Omega$ -cm. The T_c , ΔT_c , r , and ρ_0 values did not depend on film thickness in the range between 50 and 700 nm.

4.2. Results from Channeling Measurements

Channeling measurements on irradiated V₃Si single crystals provide a direct tool to determine the defect profile.¹⁷ This can be seen from the aligned backscattering spectra in Fig. 1. In this figure (110)-aligned spectra are presented prior to and after irradiation with various fluences of 600-keV Kr ions as indicated in the figure. With increasing Kr fluence the defect peak area increases. The peak maximum is found at a depth of about 120 nm, in good agreement with the calculated value (see Table I). At a Kr fluence of 1×10^{14} Kr/cm², the defect peak touches the random level, indicating that all V atoms are randomly displaced in a depth range between 50 and 150 nm. The Si atoms are also completely displaced, as can be judged from the peak height located at 400 nm in the spectrum, in comparison to the height of the Si step in the random spectrum.

Angular yield curves, which showed a narrowing of the critical angle and an increase of the minimum yield, have been taken at a depth of about 50 nm. From the narrowing of the angular yield curve the changes of the mean displacement amplitudes are evaluated using a simple analytical treatment¹⁰ and the results are summarized in Table II.

Channeling results from He-irradiated V₃Si single crystals have been discussed previously.^{10,12,17} The defect profile produced by 300-keV He ions differs from that produced by Kr ions. Here only a slight increase of the

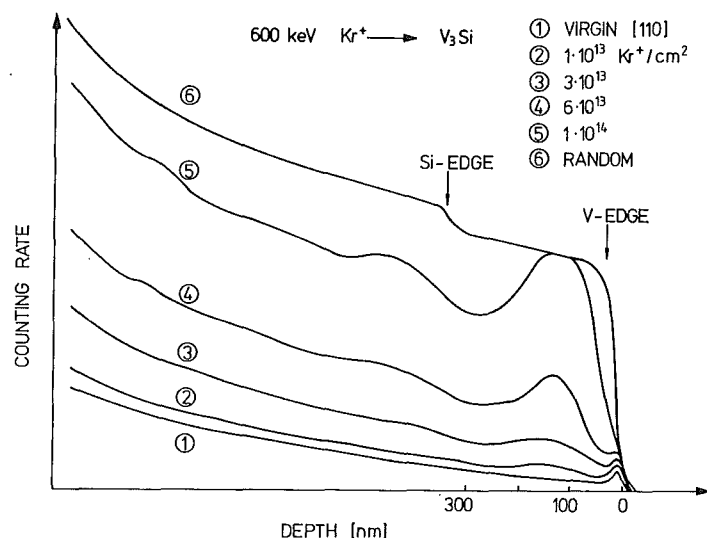


Fig. 1. Random and $\langle 110 \rangle$ -aligned energy spectra of 2-MeV He ions elastically scattered from a V_3Si single crystal. Aligned spectra are shown before and after implantation of 600-keV Kr ions at various fluences. The depth scale is calculated for He ions scattered from V atoms.

dechanneling yield was observed in the transmission region up to a depth of about 300 nm. The main damage is produced at the end of the He-ion range at about 700 nm. However, for a comparison with results from He-irradiated thin films with thicknesses below 250 nm we are only concerned with defects in the transmission region. The main defect structure in this region is made up of static atomic displacements (see Table II), which cause a narrowing of the critical angle and an increase of the dechanneling yield. A mean displacement amplitude of 0.03 Å at a reduced T_c value of 7 K was measured by Cox and Tarvin¹⁸ in agreement with the channeling data.

TABLE II

Mean Static Displacement Amplitudes (As Evaluated from Channeling Measurements) Introduced by Irradiation of V_3Si Single Crystals with Various Fluences of Kr and He Ions

Kr fluence, Kr^+/cm^2	1×10^{13}	3×10^{13}	6×10^{13}
T_c , K	10.3	3.8	1.4
$\langle u^2 \rangle^{1/2}$, Å	0.06	0.08	0.1
He fluence, He^+/cm^2	0.9×10^{16}	2×10^{16}	6×10^{16}
T_c , K	8.2	4.0	2.1
$\langle u^2 \rangle^{1/2}$, Å	0.03	0.05	0.07

4.3. Results from X-ray Measurements

Comparative integrated x-ray line intensity measurements have been performed before and after irradiation of the samples with various Kr and He fluences. In addition T_c values have been measured on the irradiated part of the samples. As an example, the intensity of the (520) line is plotted in Fig. 2 as a function of the T_c values obtained after irradiation with He and Kr ions.

It is clearly seen that in the fluence region where T_c decreases the line intensity of the Kr-irradiated sample is smaller than that of the He-irradiated sample. The x-ray lines disappear completely for Kr fluences above 2×10^{14} Kr/cm². This result is in good agreement with that obtained from channeling measurements as shown in Fig. 1, indicating that the strong disorder regions as visible in the aligned backscattering spectra after irradiation with Kr ions lead to a loss of x-ray intensity.

Little decrease of the x-ray line intensity is observed for He-irradiated samples having T_c values above 4 K. From channeling measurements we know that mainly displaced atoms with small displacement amplitudes exist in the transmission region for He-irradiated samples. More precise intensity measurements are in progress in order to investigate the influence of these slightly displaced atoms on the x-ray line intensity in the fluence region where the T_c depression occurs. For higher He fluences the decrease of the x-ray intensity is clearly seen in Fig. 2.

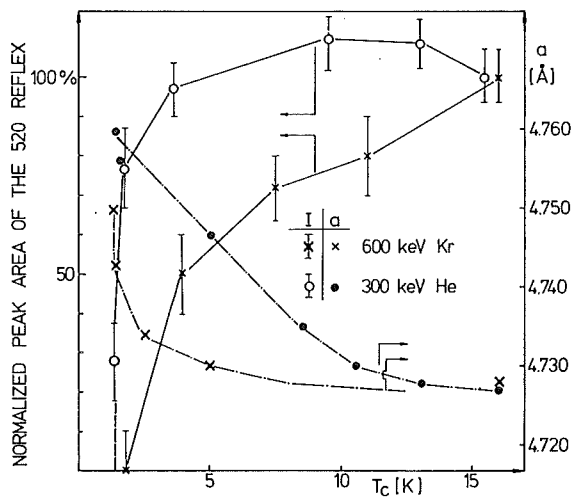


Fig. 2. X-ray integrated intensity ratio of the (520) line and the lattice parameter as function of T_c after irradiation of V_3Si layers with He and Kr ions.

Lattice parameter values are also presented in Fig. 2. In the fluence region where the strong T_c depression occurs, quite different values are obtained for He- and Kr-irradiated samples. The lattice parameter is found to increase more strongly with decreasing T_c for Kr-irradiated samples. This shows that the lattice parameter preferentially correlates with the total amount of damage rather than with T_c .

4.4. Influence of the Ion Fluence on the Residual Resistivity

From the results of the preceding sections it is obvious that the damage structure and defect density distributions are quite different for He- and Kr-irradiated samples. It is of interest to see if this difference is reflected in other properties, such as the residual resistivity ρ_0 . In Fig. 3 the change $\Delta\rho_0$ (the residual resistivity before irradiation has been subtracted) is plotted as a function of the He and Kr fluence for both polycrystalline and single-crystalline thin V_3Si films. No pronounced difference in the influence of irradiation on layers of different crystallinity can be seen. A clear difference, however, is found in the saturation value, which is about $130 \mu\Omega\text{-cm}$ for He- and about $200 \mu\Omega\text{-cm}$ for Kr-irradiated samples. The $\Delta\rho_0$ dependence on He fluence F exhibits an exponential behavior of the form $\Delta\rho_0 = A[1 - \exp(-BF)]$ (solid line in Fig. 3), where A , the saturation value, is equal to $130 \mu\Omega\text{-cm}$ and B is equal to $7 \times 10^{-17} \text{ cm}^2$. The $\Delta\rho_0$ vs F dependence for Kr cannot be described by such a formula because a second

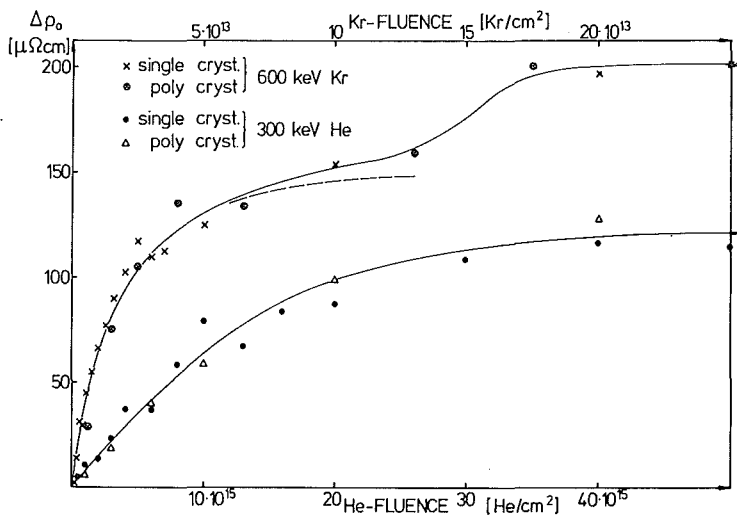


Fig. 3. Change of the residual resistivity of single- and polycrystalline V_3Si layers as function of He- and Kr-ion fluence.

damage component seems to contribute to ρ_0 in the fluence region above 1×10^{14} Kr/cm². In this fluence region the V₃Si layer becomes completely amorphous as discussed in Section 4.2. If this second damage contribution from the completely amorphous state is neglected, the measured data up to a fluence of 6×10^{13} Kr/cm², where T_c has already reached the lower saturation value, can be fitted with $A = 140 \mu\Omega\text{-cm}$ and $B = 6.0 \times 10^{-14}$ (solid line). A similar saturation value is then found for Kr and for He irradiation.

The general form of the formula for $\Delta\rho_0$ as given above is easily derived by setting ρ_0 proportional to c_D , the concentration of defects, and by calculating the rate of c_D as a function of the flux (ions/cm² sec). The saturation level is either due to an equilibrium between damage production and annealing or due to the saturation of the irradiated volume with defects.¹⁶ In order to test which mechanism would hold for the saturation process, irradiations at LN temperature have been performed with the result that no further increase of ρ_0 has been obtained for Kr-irradiated samples. In contrast, a further increase of ρ_0 was observed for He-irradiated samples, indicating that for He irradiation at room temperature the saturation of ρ_0 is due to an equilibrium between damage production and annealing.

4.5. Influence of Ion Fluence on T_c

The T_c decrease with increasing fluence is shown in Fig. 4 for Kr- and He-irradiated samples. The fluence necessary for a certain amount of T_c

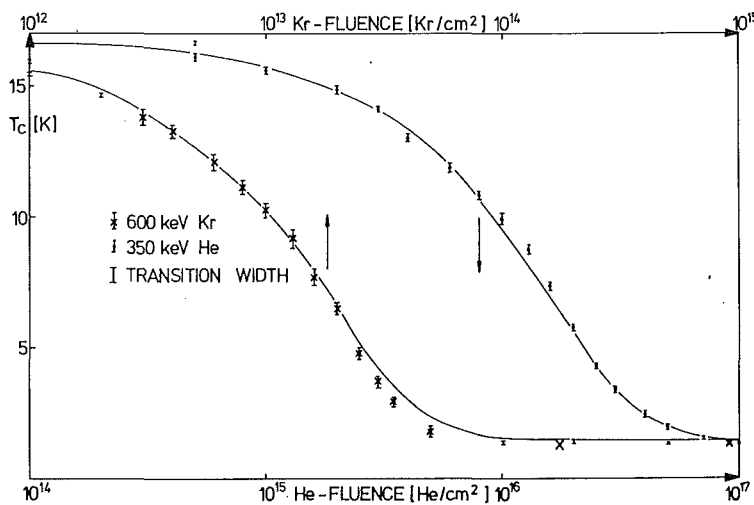


Fig. 4. Superconducting transition temperature and transition widths as a function of the He- and Kr-ion fluences.

reduction is about three orders of magnitude larger for the He- than for the Kr-irradiated sample. This difference is explained by the different energy densities deposited by He and Kr ions in V_3Si (see Table I). The saturation value is 1.3–1.4 K for He as well as for Kr ions. The width of the transition ΔT_c increases with fluence and has a maximum at a T_c value of about 9 K, with ΔT_c equal to about 0.6 K for Kr irradiation and ΔT_c equal to about 0.4 K for He irradiation. T_c decreases exponentially over the whole range of fluences for both Kr and He irradiations. The dependence of T_c on fluence is well described by an exponential term similar to that described in Section 4.4 with a constant B of about the same value for He as for Kr irradiation.

4.6. Correlation of T_c with ρ_0 and ρ_{th}

With increasing ion fluence both the resistivity at room temperature ρ_{RT} and the residual resistivity $\rho_0(T \geq T_c)$ were found to increase. In Fig. 5, T_c is given as a function of $\Delta\rho_0$ for Kr- and He-irradiated V_3Si single-crystalline films. For comparison, three values obtained from a n -irradiated bulk V_3Si single crystal have been included.¹⁹ It is clearly seen that T_c correlates with $\Delta\rho_0$ independent of the kind of radiation, although it is clear from the results of Sections 4.2 and 4.3 that different damage densities and structures exist under conditions where T_c has been reduced by similar amounts. T_c depends

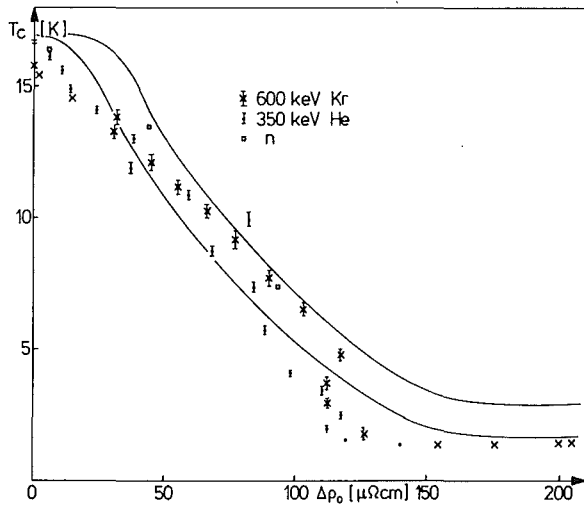


Fig. 5. Superconducting transition temperature as a function of the change in the residual resistivity after He and Kr irradiation. Included are results from a n -irradiated V_3Si single crystal¹⁹ and theoretical results (solid lines²⁰).

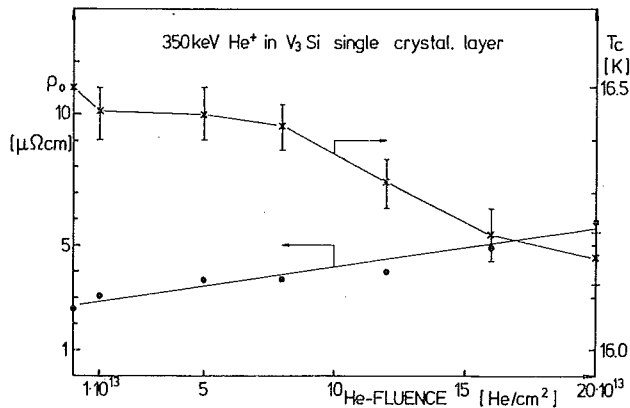


Fig. 6. Residual resistivity and superconducting transition temperature as a function of fluence.

almost linearly on $\Delta\rho_0$. This dependence is expected, as $T_c(F)$ and $\Delta\rho_0(F)$ have similar exponential dependences on F , as discussed previously.

The question arises of "threshold fluences" for both T_c and ρ_0 .¹⁹ Helium-ion irradiations of single-crystalline V_3Si films at low fluences have been performed and the results are given in Fig. 6. The residual resistivity is found to increase linearly with fluence, whereas T_c seems to be insensitive to irradiation at low fluences. This is in contrast to results from a n -irradiated bulk single crystal of similar low ρ_0 .¹⁹

In Fig. 7, T_c is correlated with the thermal part of the resistivity ρ_{th} . The T_c is found to decrease with decreasing ρ_{th} . However, we have always observed a slight increase in ρ_{th} for small fluences, and the main effect occurs after the first irradiation. An explanation for this behavior cannot be given. At high fluences, in the T_c saturation region, ρ_{th} is the difference of two large numbers $\Delta\rho_0$ and $\rho(T)$ of equal magnitude and this probably causes the fluctuation of ρ_{th} about the zero value.

A theoretical model has been developed²⁰ which combines theoretical energy-band properties for perfect V_3Si crystals and measured electrical resistivities. With this model the density of electronic states $N(E_F)$, the Fermi velocity v_F , and the plasma frequency $\Omega_p^2 \equiv 4\pi c^2 N(E_F) \langle v_F^2 \rangle / 3$ are calculated as a function of ρ_0 and ρ_{th} . Further, assuming that λ , the electron-phonon coupling constant, is proportional to $N(E_F)$, T_c is calculated as a function of ρ_0 . The results of this calculation are included as solid lines in Fig. 5. These two solid lines have been calculated assuming vibrational amplitudes corresponding to 300 and 400 K, respectively, and λ equal to 0.9 for perfect V_3Si .²⁰ In general, the agreement between measured and calculated values is good. Small deviations occur at low $\Delta\rho_0$ values, where T_c

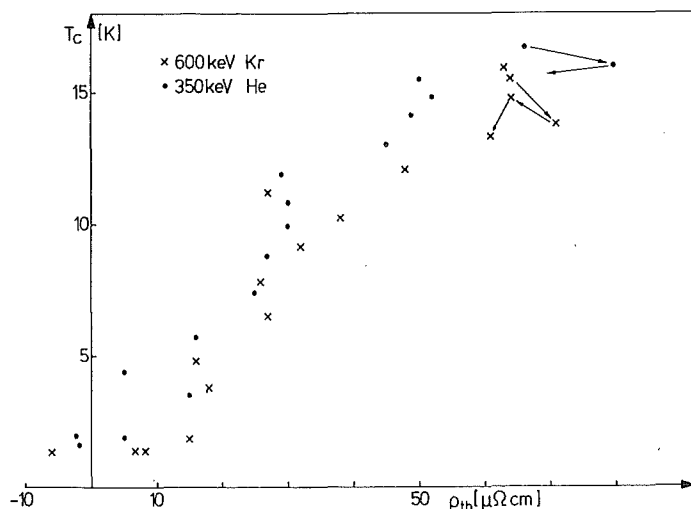


Fig. 7. Superconducting transition temperature as a function of the thermal part of the resistivity ρ_{th} .

is seen to decrease immediately with increasing $\Delta\rho_0$, in contrast to the theoretical prediction. At high $\Delta\rho_0$ values above $100 \mu\Omega\text{-cm}$ the measured T_c values are somewhat below the calculated values.

The thermal part of the resistivity $\rho_{th} = \rho_{RT} - \rho_0$ is proportional to λ_{tr} , the electron-phonon coupling transport constant, which is closely related to λ and inversely proportional to the square of the plasma frequency. For materials with the A-15 structure λ is nearly equal to λ_{tr} .²¹ We have calculated ρ_{th} under these conditions as a function of T_c using the $\Omega_p(\rho_0)$ dependence as determined in Ref. 20. A decrease of T_c with decreasing ρ_{th} was obtained in agreement with the experimental results in Fig. 7. Calculated values, however, are about a factor of 2 larger than the experimental values over the whole range of T_c .

4.7. Annealing Effects

Isochronal annealing processes have been applied to Kr- and He-implanted samples with fluences where T_c had just reached the saturation value ($5 \times 10^{13} \text{ Kr/cm}^2$, $4 \times 10^{16} \text{ He/cm}^2$) and at very high Kr fluences in the amorphous state ($1.5 \times 10^{15} \text{ Kr/cm}^2$). The results are given in Fig. 8. In the first case annealing starts at 200°C , the maximum annealing rate is reached at 630°C , and annealing is completed at 900°C . For temperatures greater than 900°C , T_c is slightly lowered and ΔT_c is broadened; for temperatures above 1000°C , T_c decreases to 2 K due to outdiffusion of Si as has been

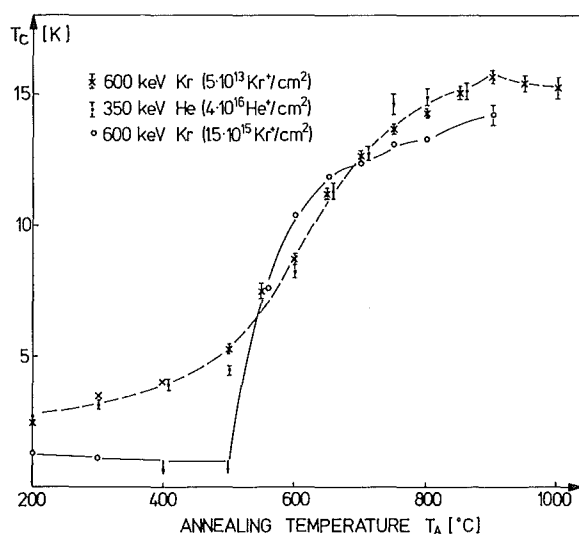


Fig. 8. Superconducting transition temperature as a function of temperature in an isochronal annealing process for samples irradiated with He and Kr ions such that T_c just reached its saturation value, and for a high Kr fluence (1.5×10^{15} Kr/cm²) in the saturation of the residual resistivity.

determined with Rutherford backscattering. In the second case, annealing from the amorphous state shows a different behavior at low temperatures, where T_c is found to decrease below the detection limit of our T_c -measuring equipment. A sudden increase of T_c is observed at 550°C, with the maximum annealing rate at 530°C. At temperatures above 650°C the annealing rate is low, and complete annealing is not yet reached at 900°C.

5. SUMMARY AND DISCUSSION

From channeling measurements on He-irradiated V₃Si single crystals it has been concluded that the main damage component (here called the first component) consists of small, static displacements of the lattice atoms with displacement amplitudes of about 6×10^{-3} nm.¹⁰⁻¹² Further, it has been shown that the maximum fraction of strongly disordered volume (amorphous zones, defect clusters, dislocations) is below 1.7% for He fluences where T_c just reached the saturation level.¹⁷

For Kr-irradiated samples a second damage component has been observed consisting of strongly displaced atoms with displacement amplitudes on the order of $1-5 \times 10^{-2}$ nm.

Comparative x-ray line intensity measurements on He- and Kr-irradiated V_3Si thin films where T_c has been reduced by the same amount reveal a stronger intensity reduction and a larger increase of the lattice parameter for the Kr-irradiated samples. This enhanced x-ray intensity loss is due to the second damage component, as demonstrated by the fact that for both x-ray and channeling experiments complete amorphization appears at similar Kr fluences ($2-4 \times 10^{14}$ Kr/cm²). Obviously this second damage component has little influence on the T_c reduction, as it is not present in He-irradiated thin films. Still, the question remains of whether the first damage component is also present in Kr-irradiated V_3Si layers. From the relative large increase of the lattice parameter for Kr-irradiated layers it can be concluded that the total irradiated volume is affected. However, a direct dependence between T_c and the lattice parameter does not exist. Thus we depend on indirect hints indicating that the first damage component does exist and that it may also be responsible for the observed T_c reduction in Kr-irradiated samples.

As T_c is measured resistively, one may assume that a reduction of T_c can only be observed if the total irradiated volume is slightly damaged. Assuming that this is the case already for a T_c depression by about 1 K, then the corresponding fluences are 2×10^{12} Kr/cm² and 5×10^{14} He/cm². On the other hand, at a fluence of 2×10^{12} Kr/cm² the volume fraction affected by the second damage component is only about 0.01 as determined from channeling measurements. This is far too small to account for the measured T_c reduction even if we were to invoke a proximity effect mechanism. A further hint arises from the T_c vs $\Delta\rho_0$ dependence, where no difference is observed for Kr and He fluences up to complete T_c saturation. This relationship indicates that a single crucial defect structure, probably displaced atoms with small displacement amplitudes, provides strong electron scattering centers. The influence of the second damage component on the residual resistivity of irradiated V_3Si samples is small for moderate fluences in the fluence region where the T_c reduction occurs. A dominant influence of the second damage component on $\Delta\rho_0$ is observed only for high Kr fluences where complete amorphization occurs.

An exponential decrease of T_c with fluence was observed for neutron irradiation experiments.² This relationship was explained by the proximity effect between observed defect clusters with low T_c and the unaffected material.⁹ We found a similar exponential behavior for He and Kr irradiation causing different damage densities and structures. The exponent in our experiment is determined by the process of damage production and saturation with fluence. These results provide a simple explanation for the observed exponential behavior of the T_c decrease with fluence.

It has been argued that the increase of the transition width with fluence would be an indication for the inhomogeneity of the damage produced by

n -irradiation.²² We observed only slight differences of ΔT_c for He- and Kr-irradiated samples, although the damage levels are quite different. As ΔT_c is not sensitive to the damage density distribution, we conclude that the second damage component in Kr-irradiated samples does not influence the T_c -depressing mechanism.

If we put together all the arguments discussed above, we may conclude that the damage component consisting of strongly displaced atoms as observed in Kr-irradiated samples is not responsible for the observed T_c reduction. In He-irradiated samples small, static displacements of all atoms is the only defect structure which has been observed. We believe that these small, static displacements are responsible for the T_c reduction. The question of the extent to which antisite defects exist and play a role in the T_c -depressing mechanism cannot be answered at present.

REFERENCES

1. Proceedings of the International Discussion Meeting on Radiation Effects on Superconductors, *J. Nucl. Mat.* **72**, 1-300 (1978).
2. A. R. Sweedler, D. G. Schweitzer, and G. W. Webb, *Phys. Rev. Lett.* **33**, 168 (1974).
3. O. Meyer, H. Mann, and E. Phrilingos, in *Application of Ion Beams to Metals*, S. T. Picraux, E. P. EerNisse, and F. L. Vook, eds. (Plenum Press, New York, 1974).
4. B. Besslein, G. Ischenko, S. Klaumünzer, P. Mueller, H. Neumüller, K. Schmelz, and H. Adrian, *Phys. Lett.* **53A**, 49 (1975).
5. L. R. Testardi, J. M. Poate, and H. J. Levinstein, *Phys. Rev. B* **15**, 2570 (1977).
6. M. Gurvitch, A. K. Ghosh, C. L. Snead, Jr., and M. Strongin, *Phys. Rev. Lett.* **39**, 1102 (1977).
7. A. R. Sweedler and D. E. Cox, *Phys. Rev. B* **12**, 147 (1975).
8. J. Appel, *Phys. Rev. B* **13**, 3203 (1976).
9. C. S. Pande, *Solid State Comm.* **24**, 241 (1977).
10. O. Meyer and B. Seeber, *Solid State Commun.* **22**, 603 (1977).
11. L. R. Testardi, J. M. Poate, W. Weber, W. M. Augustyniak, and J. H. Barrett, *Phys. Rev. Lett.* **39**, 716 (1977).
12. R. Kaufmann and O. Meyer, *Rad. Eff.* **40**, 161 (1979).
13. C. S. Pande and R. Viswanathan, *J. Phys. (Paris)* **39**, C6-389 (1978).
14. O. Meyer and R. Smithey, Kernforschungszentrum Karlsruhe, KfK 2670 (1978).
15. D. K. Brice, Sandia Lab. Res. Rep. SAND 75-0622 (July 1977).
16. M. W. Thompson, *Defects and Radiation Damage in Metals* (Cambridge Univ. Press, 1969).
17. O. Meyer, *J. Nucl. Mat.* **72**, 182 (1978).
18. D. E. Cox and J. A. Tarvin, *Phys. Rev. B* **18**, 22 (1978).
19. R. Viswanathan and R. Caton, *Phys. Rev. B* **18**, 15 (1978).
20. L. R. Testardi and L. F. Mattheiss, *Phys. Rev. Lett.* **41**, 1612 (1978).
21. N. Morton, *Solid State Comm.* **29**, 273 (1979).
22. R. Viswanathan, R. Caton, and C. S. Pande, *Phys. Rev. Lett.* **41**, 906 (1978).